Bulletin of the Seismological Society of America, 90, 5, pp. 1200–1236, October 2000

Paleoseismology of the Johnson Valley, Kickapoo, and Homestead Valley Faults: Clustering of Earthquakes in the Eastern California Shear Zone

by T. K. Rockwell, S. Lindvall, M. Herzberg, D. Murbach, T. Dawson, and G. Berger

Abstract Paleoseismic data from 11 trenches at seven sites excavated across the southern Johnson Valley, Kickapoo, and Homestead Valley faults that ruptured in the 1992 Landers earthquake, as well as the northern Johnson Valley fault which did not fail in 1992, indicate that the return period for large surface rupturing events in this part of the eastern California shear zone is in the range of 5–15 ka. The inferred slip rates, based on their respective recurrence intervals, are in the range of 0.2–0.6 mm/yr for each of the faults studied.

A previous large earthquake ruptured the southern Johnson Valley and Kickapoo faults about 5 ka B.P. The northern Johnson Valley fault also failed at about this time at 5.8 ka B.P. and may have been part of the same rupture. In contrast, the penultimate large earthquake that we identify on the Homestead Valley fault occurred about 15 ka B.P., much earlier than other faults involved in the 1992 rupture. From these observations, combined with paleoseismic work by others after the 1992 earthquake, it appears that previous events along the southern Johnson Valley and Kickapoo faults were different than those of 1992 and may have involved other fault segments. It has been over 5 ka since the most recent rupture on the northern Johnson Valley fault. Therefore, it is surprising that it did not fail in the 1992 rupture.

From our observations, dextral shear appears to be distributed across the entire eastern California shear zone, with individual faults taking only a small proportion of the overall slip. Release of this regional strain appears to occur in temporal clusters of large (?) earthquakes, with the 1992 event apparently the most recent of a sequence of late Holocene (0–1 ka) earthquakes that have ruptured the nine faults we have trenched in the southwestern Mojave desert. Previous clusters of earthquake activity occurred in the early (8–9 ka) and middle (5–6 ka) Holocene, and possibly the latest Pleistocene (~15 ka).

Introduction

The amount and extent of rupture associated with the 1992 M_w 7.3 Landers earthquake was a surprise because it involved multiple, previously mapped and unmapped faults (Sieh *et al.,* 1993) (Fig. 1). It was the largest earthquake to strike southern California in 40 years and was an order of magnitude larger than any previous historical earthquake in the eastern California shear zone (ECSZ). The largest previous historical event was the 1947 M_L 6.2 Manix earthquake (Buwalda and Richter, 1948). The Landers rupture, which propagated as two slip pulses (Kanamori *et al.,* 1992), nucleated near the southern end of a previously unmapped fault, just north of the city of Yucca Valley. Slip proceeded northward along what is now mapped as the southern portion of the Johnson Valley fault and onto the Kickapoo fault (Sieh *et al.,* 1993; in which the Kickapoo fault is named the Landers fault). Some slip also propagated northward along the Johnson Valley fault, north of its juncture with the Kickapoo fault, but surface slip died out at a minor releasing step about 6 km north of this juncture. The second subevent produced a larger amount of slip and propagated the rupture along the entire mapped length of the Homestead Valley fault, the northern half of the Emerson fault, and the southern third of the Camp Rock fault (Fig. 1). The total rupture length was about 80 km, with maximum dextral displacements of approximately 6 m recorded along the Emerson fault (Sieh *et al.,* 1993).

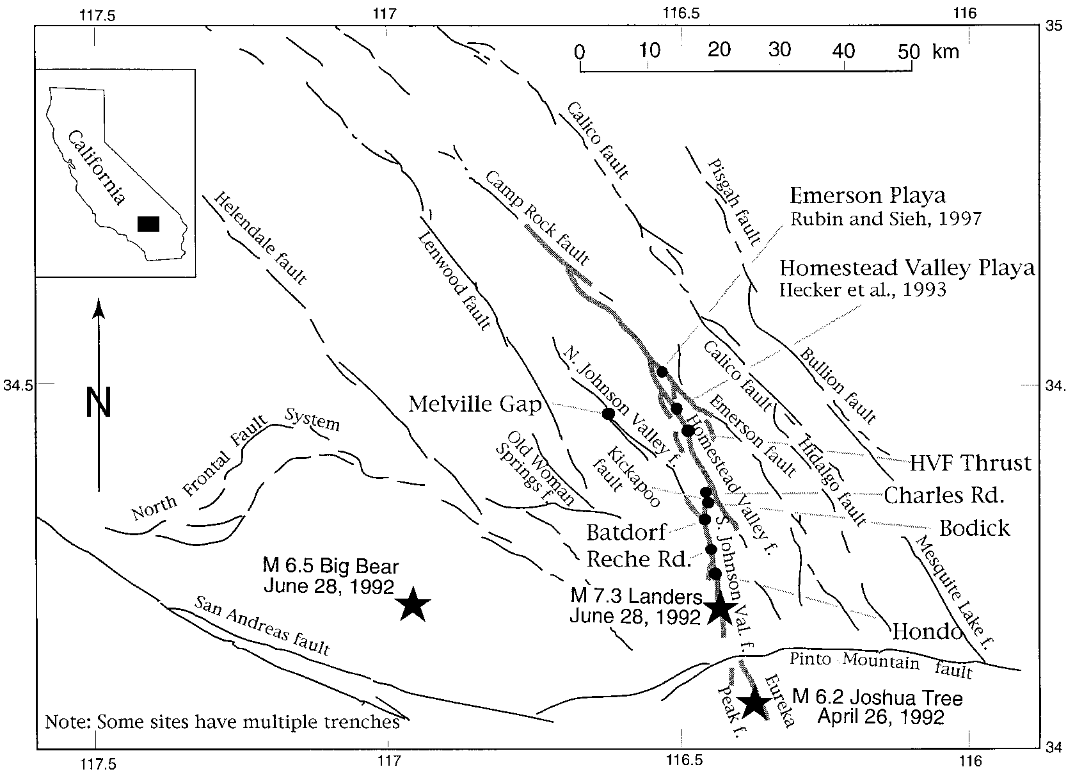

Figure 1. Faults of the eastern California shear zone in the Mojave desert of southern California (from Jennings, 1975). The 1992 Landers earthquake rupture is indicated in thick, grayed line. Trench sites are shown as black dots; we include the sites from Hecker *et al.* (1993) and Rubin and Sieh (1997) for reference.

Geodetic studies have determined that 6–8 mm/yr of dextral shear, about 15% of the Pacific–North American plate motion, is accommodated by faults of the ECSZ (Sauber *et al.,* 1986). Dokka (1983) and Dokka and Travis (1990a) have shown that individual faults have dextral displacements ranging from 1.5 to 14.4 km, with total dextral shear estimated at 65 km, all of which is inferred to have accrued during the past 10.6 Ma. The Quaternary history of these faults, however, had not been studied in detail. For the most part, previous neotectonic studies were limited to Fault Evaluation Reports (FERs) by the California Division of Mines and Geology (Hart *et al.,* 1988). The FERs identified most active fault traces associated with the ECSZ, although the 1992 rupture initiated on a strand that previously had not been considered active.

Paleoseismic investigations began within a few weeks of the earthquake (Lindvall and Rockwell, 1993, 1994; Rockwell *et al.,* 1993; Herzberg and Rockwell, 1993) to answer the following questions: (1) Did the 1992 rupture propagate northward onto the Kickapoo fault because the northern Johnson Valley fault had recently failed? (2) Was there evidence for the occurrence of similar earthquakes in the past and could we have forecast the likelihood of these five faults failing together in one large, complex event? (3) Do the Kickapoo and southern Johnson Valley faults have a common history, supporting the suggestion (Sowers *et al.,* 1994) that they are essentially the same structure? (4) What are the recurrence rates, and therefore the inferred slip rates, for faults along the 1992 rupture? (5) Is there any evidence to suggest that the late Quaternary behavior or rate of earthquake occurrence changed as a new system of faults developed, as suggested by Nur *et al.* (1993a, 1993b) and Du and Aydin (1996)? To address these and related questions, we excavated eleven trenches at seven sites along the 1992 rupture and also the northern Johnson Valley fault which did not rupture; five sites yielded useful information which we present in this article (Fig. 1). Trenches at the other two sites (Reche Road and Charles Road, which are not presented in this article) either exposed only the 1992 rupture or did not yield datable material and were not studied further.

The first question about rupture propagation focused on the possibility that a recent earthquake occurred along the northern part of the Johnson Valley fault and relieved sufficient stress to favor rupture of the Kickapoo and Homestead Valley faults. This idea was attractive because the northern half of the Johnson Valley fault is substantially better expressed in pre-earthquake aerial photography, suggesting a more recent surface rupture.

The second question addresses the feasibility of forecasting the size of future earthquakes based on study of a fault's past behavior. The observation that the 1992 rupture occurred as two subevents raises the question of whether earlier ruptures occurred as separate earthquakes, or as a single rupture sequence similar to that of 1992. We did not expect to be able to determine with a high level of confidence that two or more faults ruptured together in the past due to the inherent uncertainties in dating past events. However, it is possible to demonstrate that adjacent faults and fault segments have dissimilar rupture histories. Our findings, along with those of others (Hecker *et al.,* 1993; Rubin and Sieh, 1997) are useful in addressing this question.

The third question is whether the southern portion of the Johnson Valley fault and the Kickapoo fault are essentially the same structure. They have a common north–south strike and deviate significantly from the strike of the northern Johnson Valley fault as well as the Homestead Valley, Emerson, Lenwood, and other nearby faults. Neither the southern Johnson Valley nor the Kickapoo faults were mapped prior to the 1992 earthquake, although both exhibit some geomorphic expression in pre-earthquake photography and satellite imagery (Crippen, 1988). A plausible conclusion is that these two faults are a single structure, as suggested by Sowers *et al.* (1994). If so, then they may have a common rupture history.

The fourth issue is resolution of the recurrence rates for the faults involved in the 1992 earthquake. We also infer slip rates based on these recurrence rates, which have large errors because they are based on only two or three earthquake cycles. Understanding how slip was distributed over multiple earthquake cycles can provide valuable insights into the relative importance of individual faults in the ECSZ.

Finally, Nur *et al.* (1993a, 1993b) suggest that the 1992 rupture follows a "new" fault zone that replaces and crosscuts numerous, "older" strike-slip faults of the central Mojave region. They attribute this to the possibility that these other northwest-striking faults, along with possibly the Big Bend section of the San Andreas fault, are no longer favorably oriented to accommodate slip. Du and Aydin (1996) suggest that the development of this zone is a consequence of the development of the "Big Bend" of the San Andreas fault and has evolved relatively recently, during the past several hundred thousand years or less. If this is the case, then the faults involved in the 1992 earthquake should now accommodate much or most of the observed Mojave shear and fail much more frequently than the northwest-striking faults in the area. Although our trenching data do not extend back several hundred thousand years, the recent behavior of these faults can shed new information on their longer-term behavior and the possible implications for their evolution.

In this article, we present the results of the trenching site by site starting in the south. We then discuss the implications of our results relative to the issues raised here. We also compare our results with paleoseismic data from the Lenwood (Padgett and Rockwell, 1994), Old Woman Springs (Houser, 1996; Houser and Rockwell, 1996), and Helendale (Bryan and Rockwell, 1994) faults to the west, as well as other paleoseismic investigations along the Landers rupture (Cinti *et al.,* 1993; Hecker *et al.,* 1993; Rubin and Sieh, 1997). An unexpected result of our studies is that large earthquakes appear to temporally cluster in at least the southwestern portion of the ECSZ. Finally, a summary of the dating techniques and issues that relate to this study is presented in the appendix.

Paleoseismic Investigations Along the 1992 Rupture

Paleoseismic data are presented from the five sites along the 1992 earthquake rupture beginning with the southern portion of the Johnson Valley fault and proceeding northward along the Kickapoo and Homestead Valley faults. We then discuss our results in relation to the findings of others for the Homestead Valley fault (Hecker *et al.,* 1993) and for the Emerson fault (Rubin and Sieh, 1997).

At each site, the stratigraphic units are numbered from youngest (smallest number) to oldest (largest number), but the unit designations do not imply correlation from site to site. Further, a secondary designation is placed on most units based on the relationship to their pedogenic qualities, such as 2Ab for a buried A horizon within unit 2. We further subdivided the units with numeric subdesignations, as appropriate ($2Ab_1$, $2Ab_2$, etc.). Interpreted paleoearthquakes are given alphanumeric designations. The letters correspond to the site names (e.g., H, Hondo; MG, Melville Gap), and the numbers reflect the events recognized at each site with 1 representing the most recent event, which in most cases is 1992.

The Southern Johnson Valley and Kickapoo Faults

Four trenches were excavated at three sites along the southern Johnson Valley and Kickapoo faults (Fig. 1). The southernmost site, Hondo, is located about 200-m south of Hondo Road, which experienced about 2.9 m of offset concentrated in a relatively narrow zone of shearing in 1992 (Fig. 2). The central site, Batdorf, is located at the Batdorf residence very near the juncture of the Johnson Valley and Kickapoo faults along a strand that feeds slip to the Kickapoo fault. The northernmost of these three sites, Bodick, is located across the Kickapoo fault near Bodick Road where two trenches were excavated. Each trench exposed sediments that had been previously faulted, as discussed in this section.

Hondo Site. The Hondo trench was excavated across a discrete scarp that contained most of the 2.9 m of lateral slip and up to 40 cm of east-side-up vertical slip (Figs. 2 and 3). Additional lateral slip and up to 20 cm of east-side-down dip-slip occurred on minor strands 10–100 m west of our trench, resulting in the formation of a graben. We investigated only the eastern margin of this graben, which exhibited most of the 1992 strike slip.

The stratigraphy exposed in this trench has three primary components. West of the fault, latest Pleistocene and

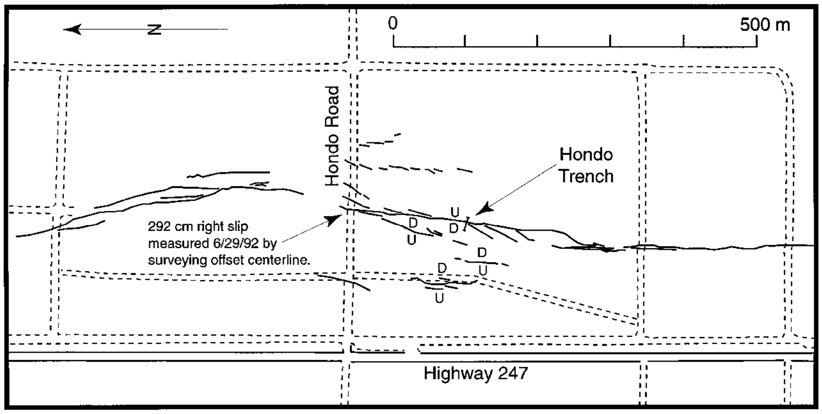

Figure 2. Map of the 1992 rupture in the vicinity of the Hondo trench site. Note that our trench did not encompass the entire fault zone, although it did cross the primary trace that sustained most of the strike slip. The area immediately west of our trench is a graben that presumably fills with sediment between faulting events, as shown in the Hondo trench log in Figure 3.

Holocene colluvial and distal alluvial fan deposits (units 1–4) overlie a sequence of Pleistocene colluvial soils developed adjacent to the fault (unit 5). The oldest deposits encountered are Pleistocene fluvial deposits (unit 6) located on the east side of the fault and at the base of the trench west of the fault (Fig. 3).

The thick section of flat-lying, stratified fluvial sediments of unit 6 east of the fault is capped by a moderately strong soil developed in the upper part of the section. The soil has an argillic horizon (Bt) with common, reddened, moderately thick clay films and an overall color of 7.5YR (Table 1). This soil has been grouped with other similar-appearing soils by Herzberg (1996) and mapped as a Q6-age deposit. Of note is the virtual lack of secondary $CaCO_3$ in this profile, which is normally associated with arid soils. Other than very minor carbonate locally superposed on the argillic horizon, there is no calcic horizon present. We presume that any Pleistocene carbonate was driven completely from the upper 2.5 m of the soil profile and that the minor carbonate superposed on the argillic horizon is of Holocene age. The lack of significant $CaCO_3$ in this profile is in marked contrast to the calcic horizons of profiles described farther northeast along the Homestead Valley, Emerson, and Camp Rock faults.

East of the fault, a stone line is present above unit 6Bt, at the base of unit 6A (the modern A horizon) (Fig. 3). The fluvial deposits exposed beneath the stone line are stone-free in the upper 1.5–2 m. This fact, along with the observation that the portion of the trench east of the fault is part of a degrading scarp (sediments dip gently east away from the fault, whereas the ground surface slopes west toward the fault), suggests that the stones were eroded from a gravelly unit that was higher in the section than is now preserved or exposed in our trench. This inference is important, as discussed later when presenting evidence of earthquake events, because clasts are now being shed off of the scarp and across the fault into the distal alluvial fan sediments west of the fault that are devoid of clasts.

A thermoluminescence (TL) sample collected from a silty horizon stratified within the lower part of unit 6C east of the fault (Fig. 3) yielded an age of 48.4 ± 6.6 ka, confirming Herzberg's (1996) inferred Pleistocene age of the soil. We use this age for both the fluvial sediments exposed in the Hondo trench, and as a control sample for the age of the Q6 deposits of Herzberg (1996).

West of the fault, units 1–4 comprise a sequence of largely gravel-free silty sand deposits, interpreted as colluvial and distal alluvial fan deposits derived largely from the west. These weakly stratified sediments have ponded against the east-side-up fault scarp. The only evidence of stratification is the presence of two buried soils in the upper 2.5 m of these deposits. Underlying these ponded deposits, unit 5 consists of two westerly dipping deposits, each with its own argillic horizon ($5Btb_1$ and $5Btb_2$). One of these deposits is wedge-shaped and is interpreted as a fault-derived colluvial wedge (unit 5Btb2). In turn, unit 5 overlies a buried argillic horizon developed in the flat-lying alluvium of unit 6 ($6Btb_3$) (Figure 3).

The buried soil of unit 4 is characterized by a dispersed, or laminar B horizon with discrete accumulations of pedogenic clay in subhorizontal bands (Fig. 3). These lamellae, each up to 1 cm thick and containing abundant translocated clay, are separated by clay-free zones of silty sand. Dispersed B horizons are fairly common in sandy, moderately- to well-sorted alluvial deposits (Dijkerman *et al.,* 1967; Torrent *et al.,* 1980), although they have not been previously described in this area. The presence of a deeply dispersed B horizon, along with the complete lack of calcium carbonate, suggests a Pleistocene age for this soil and its associated deposits. A weakly expressed contact at about a meter depth, indicated as a dashed line defining a 15-cm-thick gradational boundary on Figure 3(b) is interpreted as the top of the buried soil of unit 4. Above this, two soil profiles are present; a buried A horizon associated with unit 3 (3Ab1 on Fig. 3(b)) and the surface soil with an A horizon (unit 1A) and weak cambic (Bw) horizon (unit 2Bw).

Samples were collected for TL and photon-induced-luminescence (PSL or optical) dating from units 1, 2, and near the base and top of unit 4. The basal unit 4 alluvium yielded a weighted mean luminescence age of 25 ± 1.2 ka (Table

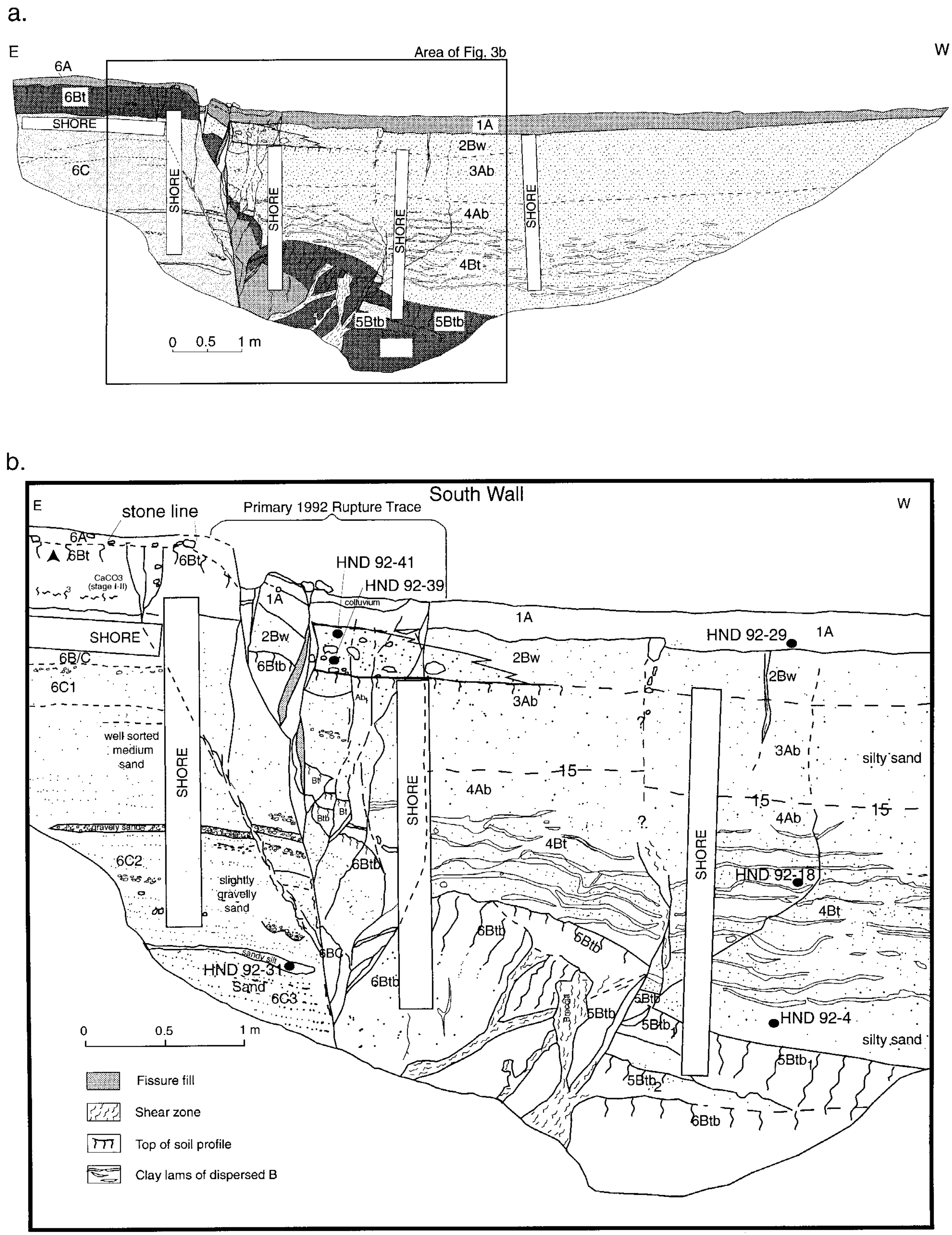

Figure 3. (a) Sketch log of the southern wall of the Hondo trench, with (b) a detail of the fault zone of the southern wall. The vertical scale in this and subsequent figures is the same as the horizontal scale.

Table 1
Landers Soil Descriptions

Pedon	Horizon	Depth (cm)	Color	Texture	Structure	Consistency	Clay Films	Carb. Stage	Bound	% Sand	% Slt	% Clay	Comments	Bulk Dens.	Clay Mass (g/cm^2)	H.I.	SDI
Hondo T-1a	A	0–13	10YR 4/4m, 5/4d	SL	1csbk	sh,so,po	n.o.	n.o.		72.74	15.77	11.49		1.42	2.1	0.25	3.3
	A2	13–22	10YR 5/4m, 5/5d	SL	m-1csbk	sh,so,po	n.o.	n.o.	73.45	15.56	10.99		1.31	1.3	0.26	2.3	
	Ab/ Colluvium	22–94	10YR 4/4m, 5/5d	LS-SL	m-1csbk	so,so,po	n.o.	n.o.	78.29	12.91	8.80		1.53	9.7	0.22	15.8	
	B lam. matrix	94–278	10YR 5/5m, 6/4d	LS	s.g.	lo-so, so,po	n.o.	n.o.		87.48	7.70	4.82		1.58	14	0.14	25.9
	B lam. lams		10YR 5/6m, 6/5d		2-3fsbk	h-shs,po	1npo,1nbr	n.o.								0.43	
	Btb	278–340 +	10YR 5/5m, 6/5d	SL	2-3vcsbk-abk	sh,so,ps	3npo, 2n-mkpf	n.o.		72.17	14.62	13.21		1.72	14.1	0.4	24.6
Hondo Pit 1	C	0–6	10YR 4/3.5m, 6/3.5d	S-LS	m-1pl	lo-so, so,po	n.o.	n.o.		86.20	11.03	2.77				0.11	0.7
	Ab	6–10	10YR 4/4m, 6/4d	LS	1-2csbk	sh,so,po	n.o.	n.o.		77.87	14.39	7.74				0.24	8
	Bw	40–115	10YR 5/4m, 5/6d	LS	1csbk	so,so,po	1cogr	n.o.		80.54	12.31	7.15				0.21	15.7
	B lam. matrix	115–216	10YR 5/4m, 5/5d	LS	lo	lo,so,po	n.o.	n.o.		85.98	7.74	6.28				0.17	17.5
	B lam. lams		7-5–10YR 5/5m, 5/6d		1fsbk	h,s,ps	1npo, 1nbr	n.o.								0.35	
	BB/Abk	216–241	10YR 5/4m, 5/6d	SL	2csbk	h-vh,s,p	3n-kpf, 2npo,1-2nbr	n.o.		73.66	13.85	12.49				0.56	14.1
	Btbk	241–281 +	7.5–10YR 4/6m, 5/6d	SL	2-3cabk	vh,s,ps	4n&2kpf, 4mkpo,2-3n-mkbr	n.o.		71.08	14.47	14.45				0.64	25.8
Batdorf	Ab	0–9.5		LS	m-1csbk & sg		n.o.		g.w	n.d.	n.d.	n.d.					
	C1	9.5–44		LS	m-1csbk & sg		n.o.		g,w	n.d.	n.d.	n.d.					
	Ck	44–90		LS	1csbk		n.o.		c,w	n.d.	n.d.	n.d.					
	C2	90–110	10YR 5/6d	S	m-sg		n.o.		a,w	n.d.	n.d.	n.d.					
	2Abk	110–131		SL	1csbk		n.o.	Stage I	c,w	n.d.	n.d.	n.d.	CaCO3 as thin porings				
	2Ck	131–146		LS	m-1csbk & sg		n.o.	Stage I	a,w	n.d.	n.d.	n.d.					
	3Ab	146–168		SL	1-2msbk		n.o.	Stage I	a,w	n.d.	n.d.	n.d.					
	3Bt	168–191	5YR 4/4d	SCL	3cpr-abk		3-4n&1mkbr, 2npf,1mkpo	Stage I	c,s	n.d.	n.d.	n.d.	CaCO3 as intraped pore linings and some pod lace linings				
	3BC	191–214		SL	1-2m-csbk		3cobr, 1nbr & po	Stage I +	n.o.	n.d.	n.d.	n.d.	Few 5–10 mm-sized CaCO3 nodules				

(*continued*)

Table 1
Continued

Pedon	Horizon	Depth (cm)	Color	Texture	Structure	Consistency	Clay Films	Carb. Stage	Bound	% Sand	% Slt	% Clay	Comments	Bulk Dens.	Clay Mass (g/cm^2)	H.I.	SDI
	3Bk	east of fault						Stage II +	n.o.	n.d.	n.d.	n.d.	Localized K fabric along bedding surfaces and faults, east of main fault				
Bodick 1	A/C	0–24	10YR5/4m, 6/4d	LS	m-1msbk & s.g.	so,ss,po	n.o.		c,i	84.49	7.55	7.96		1.79	3.4	0.183	
	Ab	24–54	10YR5/4m, 5/6d	LS	1csbk	sh,ss,po	n.o.		c,w	82.52	8.94	8.54		1.92	4.9	0.276	
	Bt/BAt	54–68	7.5YR5/4m, 5/5d	SL	2csbk	vh,vs,vp	2mkcl		c,w	73.88	8.18	17.94	Thin carb on pediaces	1.9	4.8	0.587	
	Btk	68–130	7.5YR4.5/5m, 5/6d	SL	2-3cabk	h,vs,vp	2mkcl,v1kcl	Stage I +	c,w	76.54	5.05	18.41	Stage I + w/ pore fillings & locally small nodules	2.09	28.9	0.639	
	Bk1	130–177	10YR5/4m, 7/3d	SL	2csbk	vh-eh,ss,ps	n.o.	Stage II +	c,i	64.30	21.59	14.11	Grades laterally to Stage III-	1.81	12	0.381	
	Bk2	177–203	10YR4/3m, 6/3d	S	sg + m-1fsbk	lo-so,ss,po	n.o.	I	a,w	93.35	3.72	2.93	Carbonate on scattered clasts	1.99	1.5	0.110	
	2Bk	203–215 +	10YR5/4m, 7/3d	SL	1msbk	sh,so,ps	n.o.	II-(nodules)	n.o.	68.86	23.59	7.56	Nodules to 1.5 cm	1.54	1.4	0.262	
Bodick 2	A	0–17	10YR5/4m, 6/4d	SL	1csbk	sh,ss,ps	n.o.		a,w	77.42	10.52	12.06	15 m from west well of survey profile, krotos extend down into Bt	n.d.	n.d.	0.300	
	Bt	17–59	7.5YR4/5m, 5/5d	SL	2-3cabk	h,vs,p	stains on grains	I	c-g,s	78.77	4.44	16.79	Stage I w/ filamentous pore fillings	2.04	17.8	0.520	
	Bw	69–145	7.5YR4/6m, 5/6d	S	m-sg&1msbk	h,so,po	n.o.		a,i	92.54	2.86	4.60		1.91	6.7	0.278	
	Bk1	145–198	10YR5/4m, 7/3d	LS	m-2csbk	sh,so,po	n.o.	II + to III	c-g,i	81.53	9.89	8.58	Cemented w/CaCO3	1.87	8.5	0.283	
	Bk2	198–250 +	10YR5/3m, 6/3d	S	s.g.	vh-oh, so,po	n.o.	II (pipes)	n.o.	94.88	3.04	2.08		2.06	2.2	0.189	
	A	0–5	10YR4/2.5m, 5/3.5d	LS	m-1cpl & sbk	vtr,so	n.o.		a,w	84.38	10.50	5.12					
Bodick T-2a	C	5–29	10YR4/3m, 5/4d	LS	m-1csbk	vtr,so	n.o.	No CaCo3	c,w	83.71	8.75	7.54					

	Ab	(29–44)	10YR5/4m, 5/5d	LS	1m-csbk	vtr	n.o.	No CaCo3	a,w	82.18	8.73	9.09	Note: Jan. 1993 moist, penetrated into Btb.
	Btbk	(44–82)	10YR4.5/5m, 5/5d	SL	2csbk	fr	3n & kcl, 2n & Vkbr, 2npo	I	c-g,i	76.93	7.31	15.76	
	Bwbk	(82–90)	10YR5/4m, 6/5d	LS	m-1csbk & s.g.	lo-sh	1nbr	I	a,j	86.29	5.26	8.45	Filaments CaCo3 on root casts or interstitial pores.
	K	(90–110)	10YR6/3m, 7/3d	SL	m-1msbk & s.g.	lo-h	n.o.	III		74.10	11.27	14.63	Stage III w/ cont. K fabric giving way laterally to Stage III +
	Colluvium	(0–185)											
Bodick T-2b 1/25/93	Btbk	(185–208)	7.5–10YR5/6m, 6/6d	SL	2-3csbk	vh	2-3npf, 1-2nbr, 3npo, 1mkpf	n.o.	c-g,w	74.39	9.61	16.00	Top of Bt is gone due to channeling
	Bwbk	(208–242)	10YR4.5/4m, 6/4d	LS	m-2fsbk	h-vh	1nbr & po	I	a,j	80.89	9.53	9.58	CaCO3 as fracture fillings & in pores
	BK1	(242–252)	10YR5/4m, 7/4d	LS	m-1msbk	sh-h	1nbr as a lamination	I +	a,i	82.40	8.63	8.97	CaCO3 w/a 1–3mm thick cont. CaCO3 Lam.
	K	(252–276)	10YR5/3/m, 7/2d	SL	m-2msbk	h-vh	n.o.	III −	a,w	78.17	12.49	9.34	Cont. phase CaCO3, clasts completely coated
	BK2	(276–294)	10YR5/3m, 7/2d	S	m-1csbk	h		II −		88.65	5.68	5.67	Some clasts coated w/CaCO3; may be cemented w/SiO2?
	BK3	(294–320 +)	10YR 5/3m, 7/2.5d	S	m-s.g.	lo,lo	n.o.	I	n.o.	90.75	4.49	4.76	Stage I, w/ dependent on clasts, Stage I- (locally)

(*continued*)

Table 1
Continued

Pedon	Horizon	Depth (cm)	Color	Texture	Structure	Consistency	Clay Films	Carb. Stage	Bound	% Sand	% Slt	% Clay	Comments	Bulk Dens.	Clay Mass (g/cm^2)	H.I.	SDI
HV Thrust T-1a	Av	0–2	10YR 4/2.5m; 6/3d	LS	1fsbk	so,no,po	n.o.	n.o.	a,s	n.d.	n.d.	n.d.					
	C1	2–8	10YR 4/3m;6/4d	LS	m-1fsbk-sg	so-lo,so,po	n.o.	I−	c,w	n.d.	n.d.	n.d.					
	Ck	8–51	10YR 5/3m; 6/4d	sgS	m-1csbk-sg	lo-so,so,po	n.o.	I	a,w	n.d.	n.d.	n.d.					
	Avkb	51–59	2.5–10YR 4/3m; 6/4d	sgSL	1csbk	sh-h,so,po	n.o.	I	a,w-i	n.d.	n.d.	n.d.					
	Bwkb	59–68	10YR 4/3m; 6/4d	LS-S	1msbk	so,so,po	vcogr	I	c,w-s	n.d.	n.d.	n.d.					
	Ckb	68–80	10YR 4/3m; 6/4d	sg	m-1csbk	so,so,po	n.o.	I	c,w	n.d.	n.d.	n.d.					
	2Ckb	80–98	2.5–10YR 4/3m; 5/3.5d	sgS	m-1msbk-sg	lo-so,so,po	n.o.	I	a,w	n.d.	n.d.	n.d.					
	3Ckb	98–116	2.5–10YR 4/2m; 5/3d	vgS	sg	lo,so,po	n.o.	I	a,i	n.d.	n.d.	n.d.					
	4Ckb	116–170	10YR 4/3m; 5/4d	sgtS	m-1msbk & sg	so-lo,so,po	n.o.	I−	fault	n.d.	n.d.	n.d.					
	Av	0–2	10YR		1fsbk	so,	n.o.	n.o.	a,w	n.d.	n.d.	n.d.					
HV Thrust T-2a	Bwk1	2–10	10YR	1msbk	so,	1cogr & pf	I	c,w	n.d.	n.d.	n.d.						
	Bwk2	10–21	10YR		1-2csbk	sh	2cogr	I+ to II−	c,w	n.d.	n.d.	n.d.					
	Btk	21–52	10YR		2csbk	h-vh	1nbr,2cogr,2mkcl	I	c-s,w-i	n.d.	n.d.	n.d.					
	K1	52–92			2-3cabk	vh-sh	n.o.	III+	c,w	n.d.	n.d.	n.d.					
	K2	92–130			2csbk-abk	h-sh	n.o.	II+ to III	fault	n.d.	n.d.	n.d.					
	Av	0–2	10YR		1fsbk-pl	so-sh	n.o.	n.o.	a,w	n.d.	n.d.	n.d.					
HV Trust T-2b	Bk1/Avkb	2–10	10YR	2csbk	sh,	n.o.	I	c,w	n.d.	n.d.	n.d.						
	Bk2	10–30			1msbk	so,	vcogr	I	c,s	n.d.	n.d.	n.d.					
	Bwbk	30–65			2csbk	h-vh	2cogr,vnbr	I+	c-gr,s	n.d.	n.d.	n.d					
	Bkb1	65–89			1csbk	so-sh	n.o.	I− (pockets)	g,w-s	n.d.	n.d.	n.d.					
	2bkb2	89–159			1csbk	sh,	n.o.	I− (pockets)	c,w	n.d.	n.d.	n.d.					
	3Btbk	159–190+			2csbk	h,	1-2npf,1nbr & po	II+	n.o.	n.d.	n.d.	n.d.					

Nomenclature follows Soil Survey Staff (1975) and Birkeland (1984).

Table 2
Luminescence Ages

Sample*	Depth (cm)	Feature	Dose rate (Gy/ka)	D_E† (Gy)	TL Age‡ (ka)	PSL Age (ka)	Corrected Age§ (ka)
Hondo Site							
HND92-29	15	wash sediments	6.51 ± 0.27	38.8 ± 5.7	5.96 ± 0.95		5.46 ± 0.95
HND92-29(Fs)			6.6 ± 0.2	28 ± 2[b]		4.3 ± 0.3	
				Weighted mean calibrated (HND92-29(Fs) and HND92-29) =			4.4 ± 0.3
HND92-41	25	wash sediments	6.71 ± 0.25	37.8 ± 2.1	5.63 ± 0.40		5.13 ± 0.40
HND92-39	45	wash sediments	7.09 ± 0.16	33.9 ± 1.7	4.78 ± 0.28		4.28 ± 0.28
HND92-18(Fs)	170	wash sediments	6.0 ± 0.2	100 ± 4[b]		16.7 ± 0.9	
HND92-4	270	wash sediments	6.31 ± 0.26	176 ± 20	27.9 ± 3.5		27.4 ± 3.5
HND92-4(Fs)			6.2 ± 0.2	152 ± 6[b]		24.6 ± 1.3	
				Weighted mean calibrated (HND92-4 and HND92-4(Fs)) =			25.0 ± 1.2
HND92-31	240	alluvium	5.83 ± 0.27	285 ± 36	48.9 ± 6.6		48.4 ± 6.6
Bodick Road Site							
BOD93-13	45	colluvium	7.73 ± 0.18	42.9 ± 2.5	5.55 ± 0.38		5.15 ± 0.38
BOD93-8	95	colluvium	7.81 ± 0.21	46.8 ± 2.0	5.99 ± 0.33		5.49 ± 0.33
BOD93-5	180	colluvium	6.86 ± 0.14	60.6 ± 2.5	8.83 ± 0.45		8.33 ± 0.45
Melville Gap Site							
MEL93-5	90	eolian sand	5.14 ± 0.12	31.2 ± 1.3	6.07 ± 0.35		5.57 ± 0.35
MEL93-5(Fs)			4.8 ± 0.2	29.0 ± 0.5[b]		6.1 ± 0.3	
				Weighted mean calibrated (MEL93-5(Fs) and MEL93-5) =			5.83 ± 0.23
MEL93-9	135	eolian sand	4.91 ± 0.13	39.3 ± 1.7	8.00 ± 0.45		7.50 ± 0.45
MEL93-1	195	eolian sand	4.83 ± 0.12	56.7 ± 2.6	11.71 ± 0.65		11.21 ± 0.65
Batdorf Site							
BATD94-10	170	alluvium	6.48 ± 0.15	83.0 ± 5.5	12.80 ± 0.90		12.30 ± 0.90
BATD94-3	210	buried A horizon	8.66 ± 0.31	93.9 ± 8.5	10.8 ± 1.1		10.3 ± 1.1
BATD94-1	220	buried A horizon	6.73 ± 0.17	190 ± 14	28.2 ± 2.2		27.7 ± 2.2
BATD94-8	285	buried colluvial wedge	7.41 ± 0.25	161 ± 15	21.7 ± 2.1		21.2 ± 2.1
BATD94-12	340	buried A horizon	7.41 ± 0.25	141 ± 11	19.0 ± 1.6		18.5 ± 1.6
Homestead Valley Thrust Site							
HOM92-6	60	colluvial wedge	4.96 ± 0.14	76.9 ± 5.2	15.5 ± 1.1		15.0 ± 1.1

*"Fs" indicates that sand-sized (100–200 μm diameter) K-feldspar grains were used for PSL dating. For TL dating, silt-sized (4–11 μm diameter) polymineral siliclastic grains were used. Uncertainties are $\pm 1\sigma$.

†For PSL dating, the equivalent doses were determined using 1.4 eV (880 nm, IR) excitation and measurement of the 3.1 eV (400 nm, violet) emission.

‡Ages were calculated by dividing the equivalent dose (D_E) by the dose rate.

§Corrected TL age is the TL age − 500 yrs.

2). The sample from unit 4Ab2 yielded a PSL age of 16.7 ± 0.9 ka, in stratigraphic agreement with the underlying dates. These dates indicate that the deposits into which the dispersed B horizon (unit 4Bt) is developed are about 25 ka in age and burial occurred after about 16.7 ka.

Three samples from units 1 and 2 yielded corrected ages ranging between 4 and 5.5 ka (Table 2), and indicate burial of unit 3 at that time. In that the upper two buried soils are very similar in appearance, we infer that they represent similar periods of surface exposure, or about 5 ka. Thus, the estimated age for unit 3Ab is in the range of 8–12 ka, consistent with the underlying optical age of about 16.7 ka. Collectively, the dates indicate that units 1–4 were deposited over a 20-ka interval against a rising scarp, possibly in response to discrete faulting events, as discussed later.

As shown on Figure 3(b), we have included both the argillic horizon (unit 6Bt) east of the fault and the deepest argillic horizon (unit 6Btb) west of the fault as part of unit 6, and thus have assumed that they are correlative. The correlation of these two units across the fault, which is based on their degree of soil development and the relatively horizontal nature of their uppermost contacts, provides a reasonable datum for reconstruction of slip across the main fault zone. The only possible units west of the fault that could correlate to unit 6Bt near the present ground surface are units 5Btb1, 5Btb2, or 6Btb. All three units are primarily argillic horizon material, but units 5Btb1 and 5Btb2 more likely represent local scarp-derived deposits than the underlying unit 6Btb, which is flat-lying. Unit 6Btb more likely represents a more laterally extensive soil deposit that developed on the surface of the Pleistocene alluvial fan originating from the mountains to the west.

Structural Characteristics and Interpretation of Faulting Events. The main fault is expressed as a zone of fractures that coalesce toward the base of the trench. Most of the 2.9 m of 1992 lateral surface slip occurred within a 1.5-m-wide zone with normal separation, indicated as the primary 1992 rupture trace on Figure 3. This group of fractures coalesces into a 1-cm-wide, steeply west-dipping fault at the base of the trench, which juxtaposes unit 6 alluvium on the east with down-faulted colluvial and alluvial fan material on the west. A second group of faults, about 2-m west of the primary 1992 rupture trace, appear to have accommodated a significant portion of the long-term displacement. This inference is based on the observation of relatively thick (up to 30 cm), highly sheared gouge zones, some of which are overlain by unfaulted soil units (Fig. 3). This second, western zone dips east, toward the 1992 slip surface, and exhibits reverse separation, which is the opposite sense of vertical separation as the 1992 trace. It appears to have had only minor movement during the past several events, including 1992, but obviously is a major player in the late Pleistocene history of this fault zone. The change in dip direction, with older and younger strands expressing reverse and normal separation, respectively, may indicate a local change in fault geometry, a minor change in kinematics, the direction of rupture propagation through the site, or only minor differences in the way the fault ruptured through different alluvial materials as the Pleistocene scarp was buried.

There is clear stratigraphic and structural evidence for multiple slip events exposed in this trench. Past ruptures are best displayed after the 1992 vertical separation is removed (Fig. 4(a)). In this and subsequent reconstructions, it is assumed that scarp height, as determined by topographic profiling and from trench logging, represents vertical slip. This assumption is valid if there are no significant rills or channels that have been backfilled and if the units we logged are relatively horizontal for some distance along the fault. Because the surface topography at our trench site is virtually horizontal west of the fault scarp and there is no indication of incision into the scarp for at least 10–15 m to the south, we believe this is a valid assumption. However, we cannot preclude that some of the vertical separation observed for the older units in the trench is due to buried topographic effects.

With the reconstruction shown in Figure 4(a) we removed the vertical slip in 1992 by realigning the surface topography, which required about 35 cm of restoration. After reconstruction, a buried scarp is evident in the same position as the 1992 rupture trace, which we interpret to have been produced by the penultimate event, H2 (with 1992 being event H1). The top of buried soil 3Ab retains its relatively horizontal nature to the fault, where it is juxtaposed against unit 6Bt. Because a buried A horizon could not form in this configuration, we infer that the penultimate event dropped unit 3Ab down to the west, similar to what occurred in 1992. After faulting, unit 3Ab was buried by colluvium shed from the scarp, as indicated by the wedge-shaped deposit containing abundant stones located directly west of the fault. The source of the stones is clearly the modern A horizon of unit 6 east of the fault, which exhibits a weakly formed stone line (Fig. 3(b)). This gravelly colluvium grades into the silty sand of unit 2 to the west, which we interpret as distal fan deposits derived from the west. There was no clear contact between the matrix of the colluvial wedge and the distal fan deposits, probably in part due to localized bioturbation, although the presence of the stone cluster partially delineates the contact. There apparently was sufficient time between the penultimate event and 1992 to degrade the scarp to a very subtle break in slope. Other than the broad topographic scarp degraded in unit 6 east of the fault, there was no other geomorphic indication of the presence of the southern Johnson Valley fault in this area.

TL and PSL ages of colluvial wedge material taken from between the clasts in the stone cluster and from the distal alluvial fan material several meters west of the fault are all mid-Holocene, indicating deposition of the colluvial wedge and alluvium at that time. When the corrected ages are used, the age of the stone cluster is 4.3 ± 0.3 to 5.1 ± 0.4 ka or about 4.7 ± 0.7 ka. The age of the overlying colluvial sediments is 4.3 ± 0.4 ka (Table 2), which is in stratigraphic agreement. For the penultimate event at the Hondo site, we assume the age of the colluvial wedge approximates the time of the earthquake, which therefore occurred at about 4.7 ± 0.7 ka B.P.

We used the same reconstruction procedure as before and realigned the unit 6 soil east of the fault with the top of unit 3Ab west of the fault (Fig. 4(b)), again assuming that these units are essentially horizontal and parallel to the fault. This again shows units 3 and 4 ponded against the scarp indicating prior activity. Also of note is the cluster of smaller clasts in the fault zone that are at about the same stratigraphic level as the top of unit 4Ab, which represents the second buried soil. We interpret this cluster of stones along with the burial of units 3Ab and 4 to represent the prepenultimate event, H3. The reconstruction required an additional 0.5 m of vertical slip (0.85 m total), similar to that of the 1992 earthquake.

The timing of event H3 is poorly constrained. As a rough constraint, we use the degree of soil development to estimate the ages of the deposits. As discussed in the section on stratigraphy, we estimate the age of unit 3Ab at 8–12 ka, based on the similarity of that soil to the surface deposit and soil. If this comparison is valid, then event H3 occurred about 8–12 ka B.P.

Finally, we reconstructed the top of unit 6Btb west of the fault to align with the top of unit 6Bt east of the fault, which required about 1.9 m of vertical restoration (Fig. 4(c)). This is about five times the average vertical separation of the 1992 and penultimate events. The configuration of the scarp shown in Figure 4(c) is assumed to approximate the ground surface prior to deposition of unit 4, the base of which is dated to about 25 ka B.P. Considering that each of the earlier reconstructions suggest a similar amount of vertical slip in prior events when compared to the 1992 slip, we interpret this reconstruction as representing the amount of vertical slip in five events over about the past 25 ka. This interpretation assumes a relatively planar paleotopography for 15–20 m laterally along the fault (which is plausible based on the present ground surface), and a repetition of a

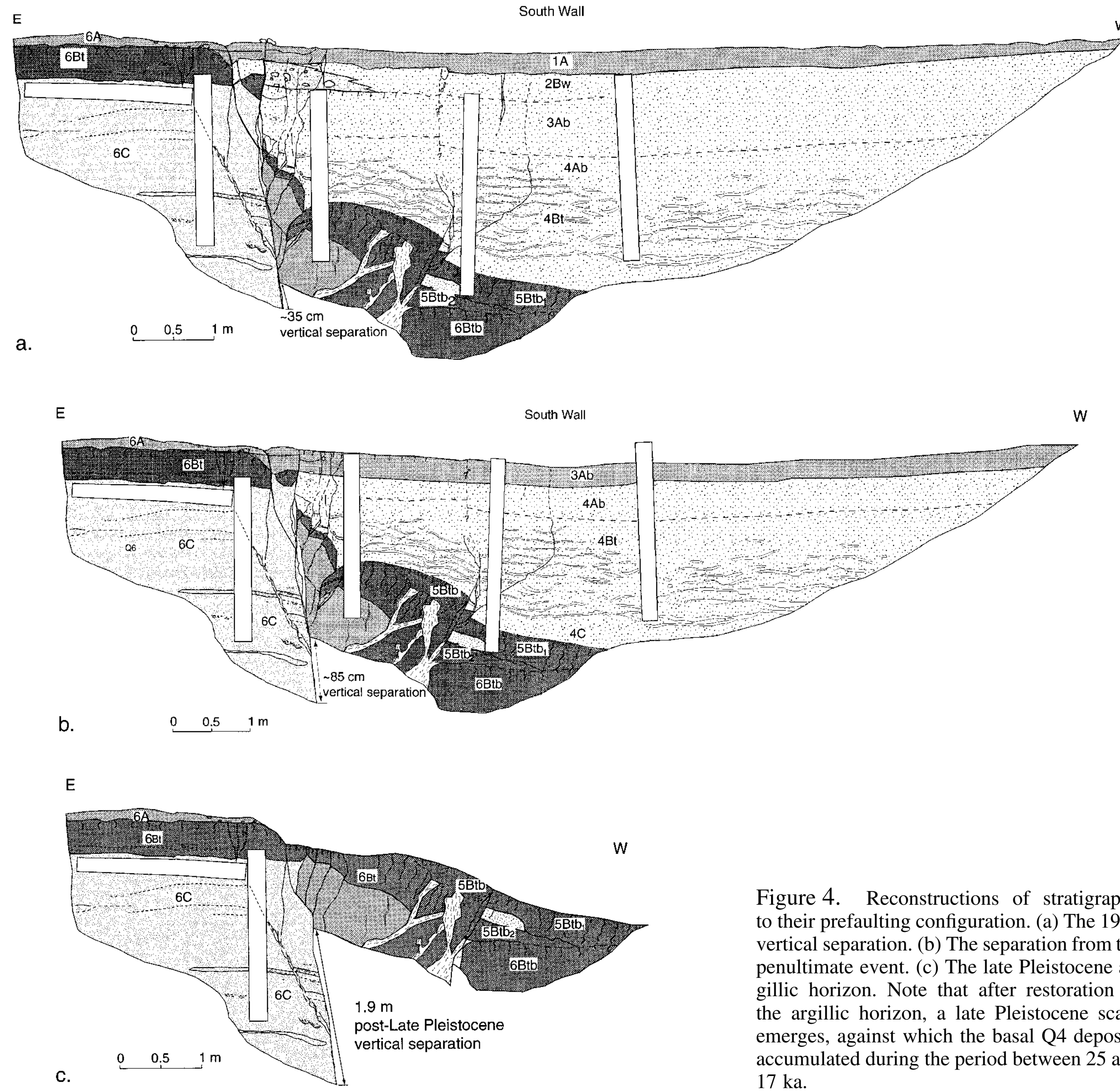

Figure 4. Reconstructions of stratigraphy to their prefaulting configuration. (a) The 1992 vertical separation. (b) The separation from the penultimate event. (c) The late Pleistocene argillic horizon. Note that after restoration of the argillic horizon, a late Pleistocene scarp emerges, against which the basal Q4 deposits accumulated during the period between 25 and 17 ka.

similar amount of vertical separation in each event. If these assumptions are true, this yields a longer-term average recurrence interval of about 5 ka. This longer-term interval is similar to the length of time between 1992 and the penultimate event, H2, at about 4.7 ka.

The Batdorf Site. We trenched along the southernmost portion of the Kickapoo fault just north of its juncture with the Johnson Valley fault (Fig. 1) in the yard of the Batdorf family. The Batdorf trench was sited in an area of complex ground rupture at the juncture of the Johnson Valley and Kickapoo Faults (Fig. 5) where only a fraction of the total 1992 slip was expressed. The site was initially excavated to evaluate the effect of rupture on the Batdorf residence as part of an investigation on how structures behave during direct fault rupture (Murbach *et al.,* 1999). Nevertheless, the stratigraphy was useful for paleoseismology, so we collected TL samples from critical stratigraphic units to constrain the timing of past events.

The sediments exposed in the trench (Fig. 6) are interpreted as debris flow and fluvial deposits derived from the San Bernardino Mountains to the west. The trench stratigraphy is described in terms of soil units, because we primarily used soil stratigraphy and the identification of buried soils to delineate the primary strata. Three primary stratigraphic units were identified, with buried soils separating each major unit. The uppermost part of the section, designated as units 1A, 1C1, 1C2, and 1C3 on Figure 6, is a

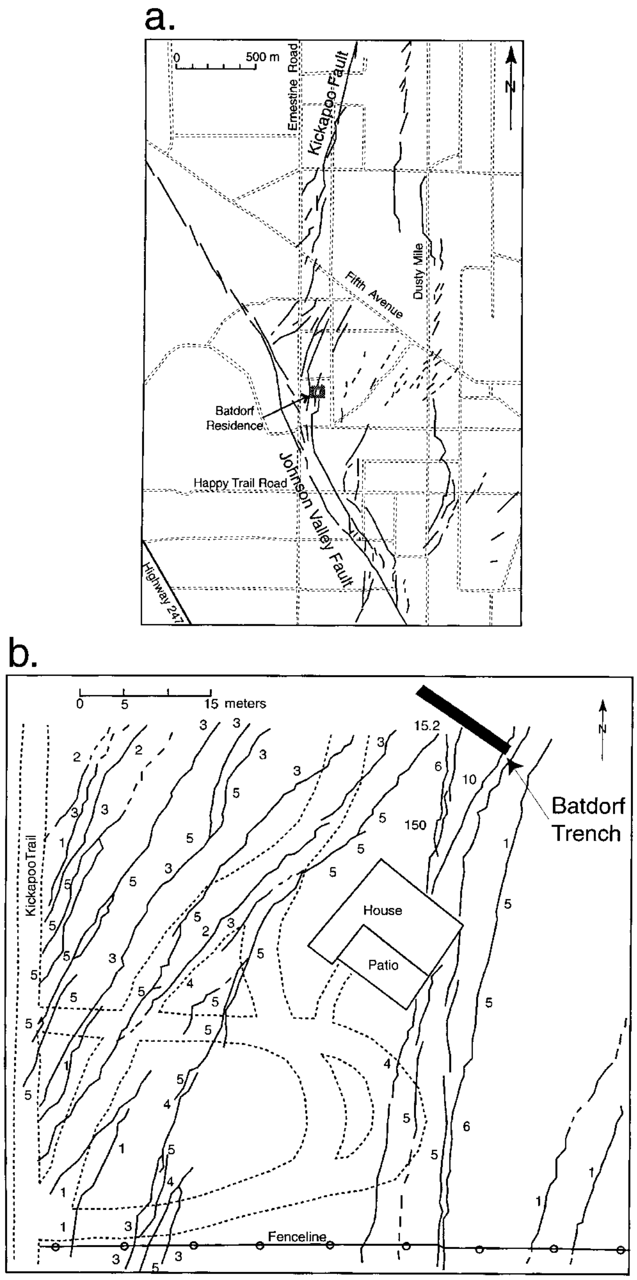

Figure 5. Map of 1992 surface rupture in the vicinity of the Batdorf residence. Note that the rupture is spread over a broad area, with right-lateral slip in cms. Also note that this trench site is interpreted to be on the Kickapoo fault, although it is virtually at the junction between the Kickapoo and Johnson Valley faults. (a) from Sowers *et al.,* 1994, (b) from Lazarte *et al.,* 1994)

slightly gravelly sand with localized gravel concentrations that exhibits channeling indicative of its fluvial origin. Other than the contact between units 1A and 1C1, which are pedogenic, all other contacts within unit C are depositional or erosional. Although the channeling has locally removed some of the underlying strata, the relatively intact character of buried soil unit 2Ab, which is about 0.5 m thick along much of the trench, indicates the absence of deep scour.

We collected one TL sample from unit 1C2 (BAT94-10) that yielded a corrected age of 12.3 ± 0.9 ka. A TL date on the underlying buried A horizon of unit 2Ab (BAT94-3) yielded a perhaps younger corrected age of 10.3 ± 1.1 ka. We infer that the older, but stratigraphically higher, date (12.3 ka) from unit 1C represents only partial bleaching of the TL signature at the time of deposition. This is expected for coarser-grained fluvial sediments, and thus 12.3 ka is a maximum age for that unit. Sample BAT94-3 was collected from a buried A horizon similar to the surface A horizon at the Hondo site from which the TL control (zeroing) samples were collected. Thus, these sediments should have been much better zeroed, or bleached, at their time of burial. Consequently, we interpret the date from unit 2Ab as the maximum age of overlying unit 1C and close to the burial age of unit 2Ab, with an age range of 9.2–11.4 ka.

Unit 2, which contains subunits 2Ab and 2C toward the west end of the trench, is a massive fine- to medium-grained silty sand that we interpret as either fluvial or debris flow in origin. There is no apparent stratification, channeling, or gravels that support the fluvial interpretation; however, we consider that option with the possibility that this is an individual overbank depositional unit. Alternatively, and probably more likely, this unit may be a deposit associated with an individual debris flow. In either case, unit 2 maintains a relatively constant thickness along the length of the trench except where it is channeled into by overlying unit 1C. A soil is developed in this unit, expressed as an A horizon over a C horizon; hence the unit designations of 2Ab and 2C.

Unit 3, with subhorizons 3Ab, 3Bt, 3BC/Bw, and 3Bk represent a relatively strong soil developed in a poorly stratified silty sand deposit. Unit 3BC is stratigraphically contiguous with unit 3Bk, although substantial amounts of secondary calcium carbonate overprint the deposit east of the fault in unit 3Bk.

The soil developed in unit 3 (Table 1) exhibits a moderately developed argillic (Bt) horizon with many thin to moderately thick reddened clay films, strong angular blocky to prismatic structure, and an overall dry color of 5YR 4/4. Unit 3Bk is interpreted as the associated calcic horizon for this soil profile with stage II+ development and localized K fabric along bedding surfaces and faults. This soil is similar in development to the Q6 soils mapped by Herzberg (1996) and at least as well-developed as the Q6 soil exposed in the Hondo trench, so we infer a similar, but probably slightly older, late Pleistocene age for this deposit of 50–100 ka.

We collected one sample for TL analysis from unit 3Ab (BAT94-12), from west of a buried fault scarp (Fig. 6), that yielded a corrected age of 18.5 ± 1.6 ka (Table 2). A wedge-shaped deposit, indicated as unit 2col on the trench log (Fig. 6) buries a paleofault scarp and is interpreted as a fault-generated colluvial wedge. The wedge material directly buries 3Bt soil material exposed in the scarp face and is com-

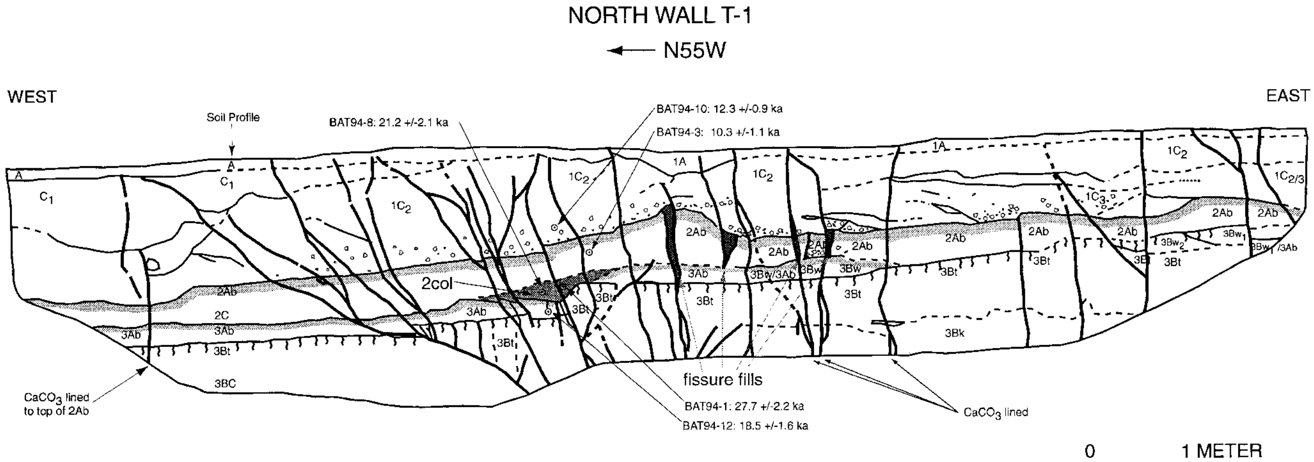

Figure 6. Log of the north wall of the Batdorf trench. Light shading indicates the presence of a buried A horizon. Medium and dark shading are deposits interpreted to be a colluvial wedge derived from erosion of a fault scarp and fissure fills, respectively.

posed of material eroded from both the 3Ab and 3Bt units. We attempted to directly date this wedge with TL (samples BAT94-1 and BAT94-8; Table 2), although with limited success. The resulting ages of 27.2 ± 2.2 ka and 21.2 ± 2.1 ka are older than the date from the underlying unit 3Ab, although BAT94-8 is only slightly older. Although we attempted to locate the sample in an area with no chunks of eroded 3Bt material, we interpret the 27 ka result to mean that some eroded argillic material, with an apparently significant inherited age, was present within the sample matrix, thereby producing the obviously too-old age. Thus, the only direct age constraints on the colluvial wedge are bound by the dates on units 2Ab (10.3 ka) and 3Ab (18.5 ka), although the actual age is probably close to that of 3Ab, a buried A horizon.

Paleoearthquake Events. We recognize evidence for three surface ruptures in the Batdorf trench: one in 1992 and two previous events. The effects of the 1992 rupture are ubiquitous, with shattering of the strata in an upward flowering zone of fractures (Fig. 6). Notably, no scarp was produced at the surface, and the slip was distributed across the entire zone of fractures, although some cracks exhibited significantly greater displacements at the surface than others did.

The two paleoevents were recognized from both structural and stratigraphic observations. The penultimate event, BA2, is interpreted from a number of fissure fills and minor scarps that are present in unit 2Ab but are truncated by the overlying channels and strata of unit 1C. Some of the fissure fills, located near the center of the trench (Fig. 6), are as wide as 10–15 cm where they are truncated by unit C alluvium. We also observed that many of the fractures, some of which rebroke in 1992, are lined with $CaCO_3$ up to the top of the 2Ab surface, which we interpret to be the result of prior fracturing up to that paleosurface. From these observations, we infer that a surface rupture producing fractures similar to that of 1992 occurred when unit 2Ab was at the surface. Using the TL dates on that unit as discussed earlier, that faulting event (BA2) is poorly dated and occurred after 9–11.6 ka but before unit C was deposited. In that 2Ab is an A horizon, the burial age, and therefore the age of the earthquake, is probably close to 9 ka.

The third event we recognize apparently produced a scarp in the unit 3 deposits just west of the middle of the trench, which was subsequently buried by the wedge of material we interpret as an event-generated colluvial wedge. Here, the 3Ab horizon is dropped down to the west against the 3Bt horizon. The 3Bt is rounded and degraded at the fault, and overlain by the colluvial wedge, all indicating degradation of a surface scarp. Thus we infer the event occurred while 3Ab was at the surface, prior to deposition of unit 2. The age of unit 3Ab, based on the TL date discussed earlier, is about 18.5 ± 1.6 ka, which we infer as the maximum age of the third event, BA3. In that unit 3Ab is a buried A horizon, and based on the observations that A horizons tend to be fairly well-zeroed with respect to residual TL signatures, we infer BA3 to have occurred at about 18 ka.

From the observations and dates of soil units in the Batdorf trench, we conclude that there have been only three surface ruptures in the period between about 18.5 ± 1.6 ka and 1992. The penultimate event occurred after the period of 9–11.6 ka. From these data, the return time for large earthquakes that rupture the Kickapoo fault appears to be on the order of about 8–10 ka, longer than that inferred for either the southern or northern portions of the Johnson Valley fault.

The Bodick Trench Sites. The first trench we excavated along the Kickapoo fault was located a few meters south of Bodick Road where 2.5 m of lateral slip was observed in 1992. The trench exposed a well-developed soil with a reddened argillic horizon that correlated to Herzberg's (1996) Q6 group of deposits. However, very loose, friable, coarse sand was present below the argillic horizon that collapsed when the trench was opened. Further, the presence of an old soil at the surface immediately indicated that no deposition had occurred in that area for a long time, perhaps many tens of thousands of years. Consequently, we did not consider this a useful trench for paleoseismic study, especially in light of its hazardous condition, and did not log it in detail. Nevertheless, we did describe the soil (Table 1) and made a few observations about the trench that indicate repeated failure during or after soil development.

We observed the presence of a calcic horizon at depth below the argillic horizon, indicating insufficient moisture during the late Pleistocene in this area to completely flush the carbonate from the profile. We also observed minor $CaCO_3$ superposed on the argillic horizon that we interpret to be Holocene in age. In the fault zone, fractures were observed to be heavily lined with calcium carbonate up into and near the top of the Bt horizon. Considering the clear bimodal distribution of carbonate, which we interpret to represent the differences between Pleistocene and Holocene climate as inferred elsewhere in the Mojave region (Machette, 1985; McFadden, 1988), we interpret all of the carbonate in the argillic horizon, including that in the fractures, as Holocene in age. Because carbonate linings of fractures require the preexistence of the fractures, we infer that the Kickapoo fault at this site has experienced prior Holocene rupture to account for the production of fractures that were subsequently filled by the Holocene carbonate. If the event occurred in the late Pleistocene when rainfall was higher, there would likely have been sufficient time to heal the fractures in the expansive clay medium of the argillic horizon. The fact that the fractures appeared to be open and simply lined with carbonate implies that the fractures themselves are Holocene.

We then searched for a more favorable site for a second trench along the Kickapoo fault, where late Pleistocene and Holocene sedimentation has occurred, and chose a site about 0.2 km south of Bodick Road in an area of rilling and active alluviation. As before, the subsurface materials were found to be very sandy and would not sustain a deep trench face. Consequently, we benched the trench at an overall 1:1 slope (benches the same width as the bench faces) for stability. Even then, it was difficult to avoid collapsing individual benched faces, so we used plywood on the benches to distribute our weight.

We excavated three benches for a total trench depth of about 3 m. A reddened Q6 soil, interpreted to be late Pleistocene in age, was exposed along the entire length of the trench, which provided a correlative unit across the fault zone. The trench exposed the northern margin of an old swale in the uppermost northern bench face (Fig. 7). Therefore, the paleoground surface represented by the reddened soil was not flat at this site and our dip-slip reconstructions of that datum will be flawed.

We exposed three principal alluvial units in this trench. The oldest is a stratified, locally gravelly sand capped by a strongly developed Q6 Pleistocene soil, designated as unit 3 on Figure 7. As before, subunit designations follow their respective pedogenic horizons (i.e., A, Bt, K, and C). This Pleistocene unit is in turn incised by a channel that is backfilled with gravelly sand of unit 2 on the western (hanging wall) side of the fault. Units 2 and 3 are both overlain by a massive silty sand (unit 1) that we interpret as fluvial deposits, which thickens across the fault to the east.

Understanding the location of the soil horizons and deposits logged on Figure 7 requires the recognition that the soil is partially developed down into the aforementioned channel. West of the fault, the argillic horizon (unit 3Bt) of the Pleistocene soil is exposed in the uppermost face (face 1; Fig. 7), and immediately overlies a stage III calcic horizon (unit 3K) of which only the top 10–15 cm is exposed. Unit 3 is not exposed in face 2 of the trench because it has been locally channeled and backfilled with the younger, massive gravelly sand of unit 2. In the 2-dimensional log (Fig. 7), unit 2 appears to be below unit 3, although this is simply because unit 2 on face 2 is in front of unit 3 on face 1 from the perspective of the middle of the trench.

The expression of the argillic and calcic horizons developed in unit 3 (Table 1) clearly indicate the strength of the soil profile, which when compared to the Hondo site and other Mojave soils, required 50–100 ka of time to develop. In contrast, unit 2 has virtually no secondary carbonate, suggesting a significantly younger age than unit 3.

In the third and lowermost trench face, a cobble-rich gravel unit defines the base of the channel deposits of unit 2 and is observed incising and cutting out the lower part of the calcic horizon, which here expresses stage II development. This calcic horizon is essentially the lower part of the same profile exposed in the top bench (Fig. 7). Thus, the paleochannel incised to about 2.5 m below the level of the modern surface, and was backfilled with gravelly sand, at least on the hanging-wall side of the fault. We did not encounter this unit on the east side of the fault, almost certainly due to its strike-slip displacement out of the area of our trench.

Overlying units 2 and 3 soil is the massive silty sand deposit of unit 1 that thickens to the east across the fault. Very weak stratification is present within the upper half meter east of the fault. Unit $1C_{1a}$ is thickest at the fault and generally thins to the east, away from the fault. This unit is interpreted as either a colluvial deposit shed from the scarp after the penultimate event or alluvium buttressed against the scarp. Several strands of the fault break to the base of unit $1C_{1a}$ but do not offset it; none of these faults were reactivated in 1992 (Fig. 7(b)). This unit is capped by a thin A horizon but expresses no other pedogenic development, implying a Holocene age.

Three TL samples were collected from the silty sand of unit 1: two from below the colluvial wedge (unit $1C_2$) and one from within it (unit $1C_{1a}$) (Fig. 7; Table 2). All three TL dates yielded consistent results in expected stratigraphic order. The base of the silty sand yielded a corrected date of

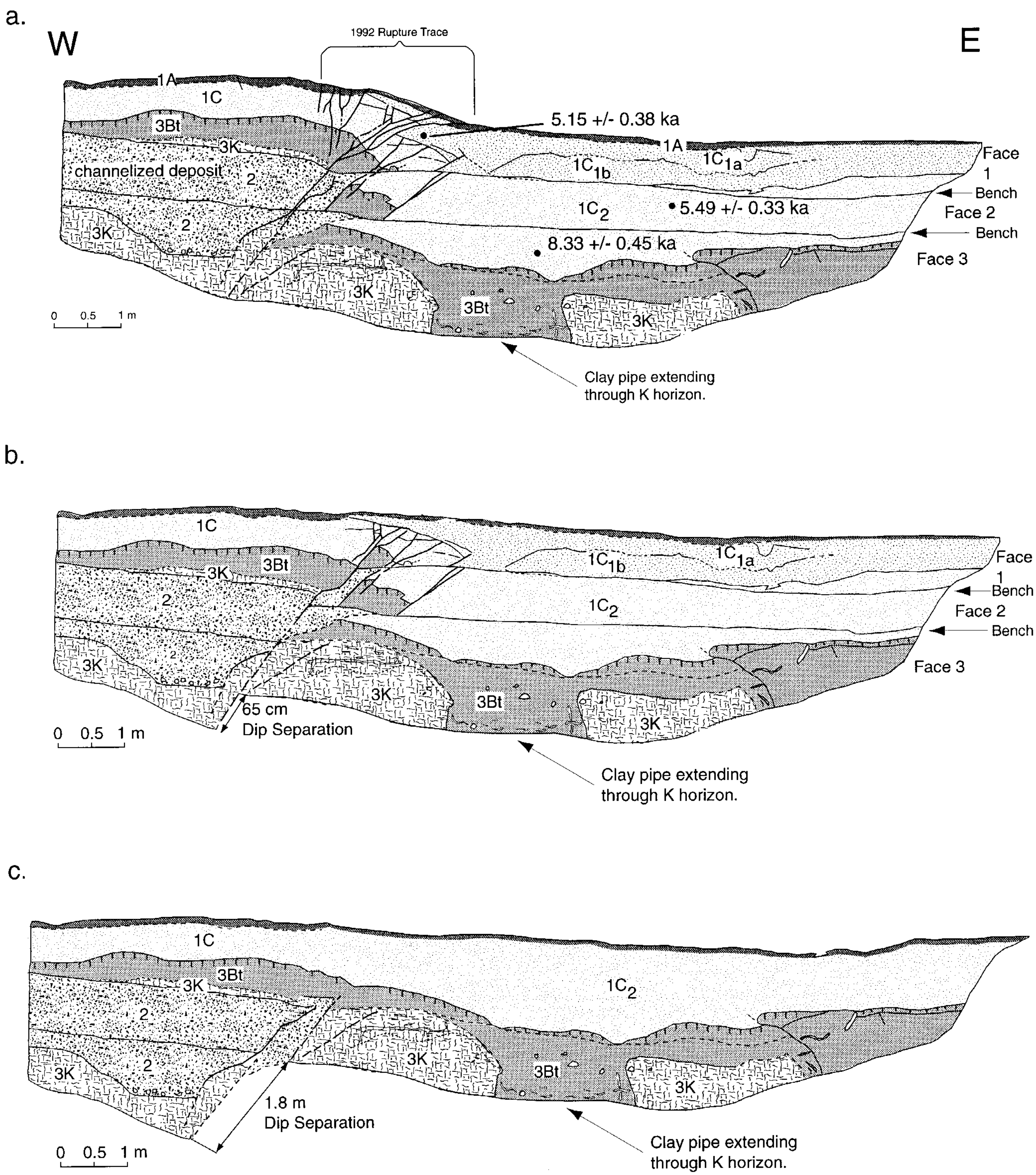

Figure 7. Log and reconstructions of the north face of the Bodick trench. (a) the initial trench log; (b) the ground surface prior to the 1992 earthquake; (c) the inferred ground surface prior to the penultimate event.

8.3 ± 0.45 ka, indicating that unit 1 is Holocene in age, consistent with the absence of much pedogenic development. The top of unit $1C_2$ yielded a corrected age of 5.5 ± 0.3 ka, and unit $1C_1$ gave an age of 5.2 ± 0.4 ka. These TL ages indicate deposition of unit 1 during early to middle Holocene time.

Faulting Events. At least three faulting events are recognized from the Bodick trench based on both structural and stratigraphic observations. Event BO1 broke to the surface in 1992, displaced the A soil horizon of unit 1, and produced about a half meter-high rounded scarp (Fig. 7(a)). The rounding of the scarp is due to the rollover of the fault in the upper half meter rather than diffusion off the scarp face. We reconstructed the 1992 vertical slip by unslipping the faults to realign the base of unit $1C_{1a}$, which required about 65 cm of dip restoration (Fig. 7(b)). This nearly removed the surface scarp; we interpret the slight remaining surface inflection as the degraded scarp from the penultimate event.

The penultimate event (BO2) is easily recognized in Figure 7(b) by the many fault strands that break unit $1C_2$ but do not penetrate up into unit $1C_1$. Unit $1C_1$ abruptly begins at the fault and buries the previous scarp. We interpret the event horizon as the lower contact of unit $1C_{1a}$. The two upper TL ages bracket the age of event BO2 to be between about 5.5 ± 0.3 ka and 5.2 ± 0.4 ka, or about 5.3 ± 0.5 ka B.P.

Further reconstruction to remove the vertical separation from the penultimate event was attempted by restoring both the top and base of unit $1C_2$ and the buried argillic horizon (Fig. 7(c)), which required about 1.8 m of dip restoration. We did not include unit $1C_1$ in Figure 7(c) because it postdates the penultimate event. The amount of restored vertical separation is about 2.75 times the 1992 vertical separation. This may indicate that the penultimate event was about 75% larger, at least in terms of vertical separation. This is consistent with our observations at the Hondo site that the penultimate event, also dated to about the same time (4.7 ka), was about 45% larger than that which occurred in 1992. We discount the possibility that two events produced the buried scarp because there is neither any structural nor stratigraphic evidence to support such an event. Nondeposition between earthquakes is always a possibility but the nearly identical ages of the sediments of unit $1C_2$ and the overlying unit $1C_1$ seem to preclude this option.

There is a minor fault strand with opposite vergence east of the main fault zone that did not rupture in 1992. This fault breaks the top of the buried argillic horizon into unit $1C_2$ but could not be followed upward due to the massive nature of unit 1. We interpret this strand to also be due to movement during the penultimate event, although we cannot preclude that this represents an earlier surface rupture at or slightly younger than about 8 ka, the age of the lower portion of unit $1C_2$ which is faulted by this strand.

Another possible explanation of why the penultimate event appears larger is that lateral slip (about 2.5 m on this strand in 1992) may have amplified the apparent separation by juxtaposing topographically higher and lower portions of the buried argillic horizon. However, the trench was excavated in the axis of the channel on the west side of the fault, so lateral slip should have decreased the amount of vertical separation with right-lateral slip, not amplified it. Nevertheless, because there may be other buried depressions, and we do not know the subsurface extent of these units, lateral juxtaposition remains a possibility to explain the greater apparent vertical separation.

At least one earlier event is suggested by two lines of evidence. First, the reconstruction shown in Figure 7(c) still leaves a buried paleoscarp present at its time of burial at about 8 ka. Second, at least one fault strand was observed on the footwall of the 1992 rupture that breaks unit 3 material but does not penetrate the buried argillic horizon nor displace units 1 or 2. This event is interpreted to be late Pleistocene in age to allow for reformation of the argillic soil over the fault strand, although there are no direct age constraints.

In summary, the Kickapoo fault has clearly ruptured twice in the Holocene with the pre-1992 event having occurred at about 5.3 ka. The penultimate event may have been larger, at least in terms of its vertical component of slip. There is permissive evidence that an earlier Holocene event occurred, although we think this is less likely. After reconstruction of the Holocene displacement, it is clear that a scarp was present in the Pleistocene alluvial deposits, indicating recurrent faulting back into at least late Pleistocene time.

Northern Johnson Valley Fault

We explored two possible trench sites along the northern portion of the Johnson Valley fault, which did not rupture in 1992, during the months after the 1992 earthquake. One site, herein named the Means Lake site, is located about 4 km northwest of the northern termination of 1992 slip, where a small arroyo draining to Means Lake has incised the desert floor (Fig. 8). We cleared the arroyo wall and located the fault, but determined that the stratigraphy is poorly layered and datable material was scarce (Bornyasz, 1993). Consequently, the Means Lake site was not pursued.

The second site, herein named the Melville Gap site, is located north of a major system of pressure ridges comprised of uplifted bedrock, along a drainage that feeds into Melville Lake (presently a playa) (Fig. 8). A shallow arroyo has incised about a meter into eolian sand and well-bedded fluvial and lacustrine (?) deposits, and abundant detrital charcoal is preserved in the strata. Hence, this site looked considerably more promising than the Means Lake site, and we chose to concentrate our efforts here.

The Melville Gap Site. We excavated a several-hundred-meter-long trench across the two vegetation lineaments that are observable in the 1954 aerial photography (Fig. 8). The trench exposed well-bedded stratigraphy to a depth of nearly 3 m (locally), and a well-expressed fault zone spanning the

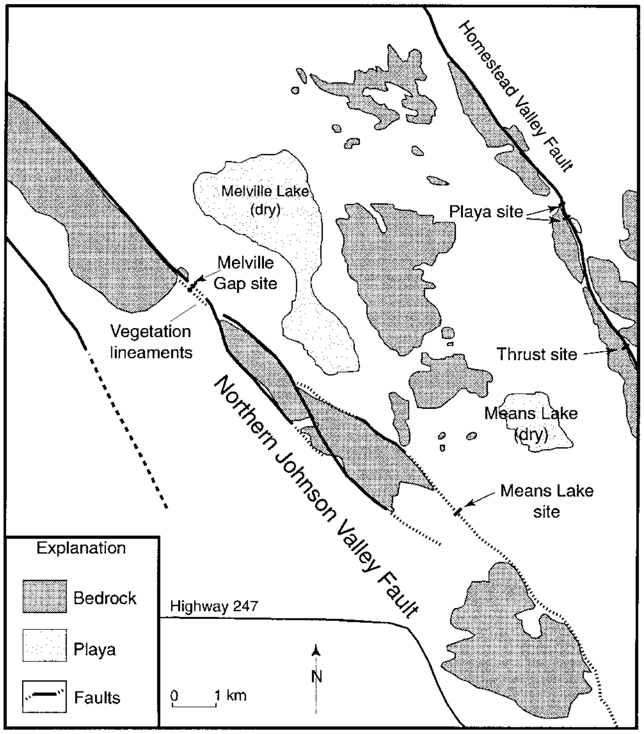

Figure 8. Map of the northern Johnson Valley fault (from Bornyasz, 1993; Herzberg, 1996) showing the Means Lake and Melville Gap sites. Faults are dashed where approximately located, dotted where concealed.

eastern lineament (Fig. 9). The western lineament is probably the result of a ground-water barrier produced by a buried fault, although the fault does not rupture or deform the upper several meters of stratigraphy and was not studied further.

The main fault zone, as shown on Figure 9, is nearly 15 m in width with a primary strand on the west bounding a graben that drops the stratified sediments by about a half meter. The stratigraphy is warped back up to the east such that the overall sense of vertical separation across the entire 15-m-wide zone is up on the east (Fig. 9). The eastern side of the graben contains many small fractures and faults but most of the deformation appears to be accommodated by folding. Some of the fractures terminate at different levels, which may indicate recurrent faulting, as discussed in this section.

The section of detailed stratigraphy was differentiated into six primary mapping units and further divided into 31 distinct strata. Only the six primary units are labeled on the trench logs in Figure 9. Unit 1 is a massive sand interpreted to be of eolian origin because dune forms are present at the ground surface. This dune sand overlies unit 2, a section of interbedded clay, silt, and sand that is restricted to the vicinity of the fault zone. Unit 3 is a sequence of finely bedded fluvial strata to the west that grade eastward into massive sand of presumed eolian origin. This unit is also restricted in its distribution by the eastern margin of the fault zone, indicating tectonic control of sedimentation.

Unit 4 is also a finely bedded section composed of fluvial overbank silt and sand that extends across the entire length of the trench (Fig. 9). It is differentiated from unit 3 by an angular unconformity in the eastern half of the fault zone. Unit 5, which underlies unit 4 across the entire length of the trench, is a massively bedded gravelly sand of presumed fluvial origin. The lowermost unit (unit 6) exposed in the Melville Gap trench is a massive, highly calcareous silty sand deposit of possible playa origin.

Charcoal was distributed throughout unit 1 and the thinly bedded section of units 3 and 4. Six samples were submitted for ^{14}C dating analysis from units 3 and 4, and one sample was also submitted from the eolian deposits of unit 1 (Table 3). All of the samples from the bedded section of units 3 and 4 yielded ages that are within a few hundred years of each other, between 9 and 9.5 ka in calendar years. One could deduce from this that the entire section of units 3 and 4 was deposited in a few hundred years or less, which is possible. An alternative hypothesis is that the charcoal was reworked from a common source of a very limited age range. In order to provide additional age control for this section, we collected and analyzed three samples for TL dating from units 3, 4, and 6, one of which was also used for PSL dating (Fig. 9; Table 2). The TL and PSL ages for the samples from units 3 and 4 are significantly younger than those of the detrital charcoal samples, being 5.8 $\pm$ 0.2 ka for the upper part of unit 3 and 7.5 $\pm$ 0.5 ka for the lower part of unit 4. An age of 11.2 $\pm$ 0.7 ka was obtained for the upper part of unit 6.

Disregarding any effects from uncorrected unstable luminescence (discussed later), our multialiquot TL and PSL dating procedures provide maximum ages for the materials tested because there is always the possibility of insufficient light exposure before burial. Because the sunlight exposure requirements are very different for the two techniques (Aitken, 1998), the agreement between the two ages for the unit 3 sample (MEL93-5; Table 2) indicates that the daylight exposure was adequate for this sample. Radiocarbon dating also provides maximum ages because charcoal dates represent the time of wood growth, which is always older than the time of deposition. However, charcoal may be resident in a system for an extended period of time, especially in arid regions. Rubin *et al.* (1998) documented variation by up to 15 ka of ^{14}C charcoal ages within the same horizons of colluvium from the Los Angeles area, and attributed this variation to incorporation of older charcoal into younger deposits by downslope reworking. Similarly, in an area southeast of Los Angeles, Vaughan *et al.* (1999) documented charcoal ^{14}C ages that were 5–8 ka older than grass-blade ^{14}C ages from the same peat horizons, indicating substantial residency of detrital charcoal within the drainage system. The results from the grass blades provided the most accurate ages for the peat beds.

For our Melville Gap site, we conclude then that the

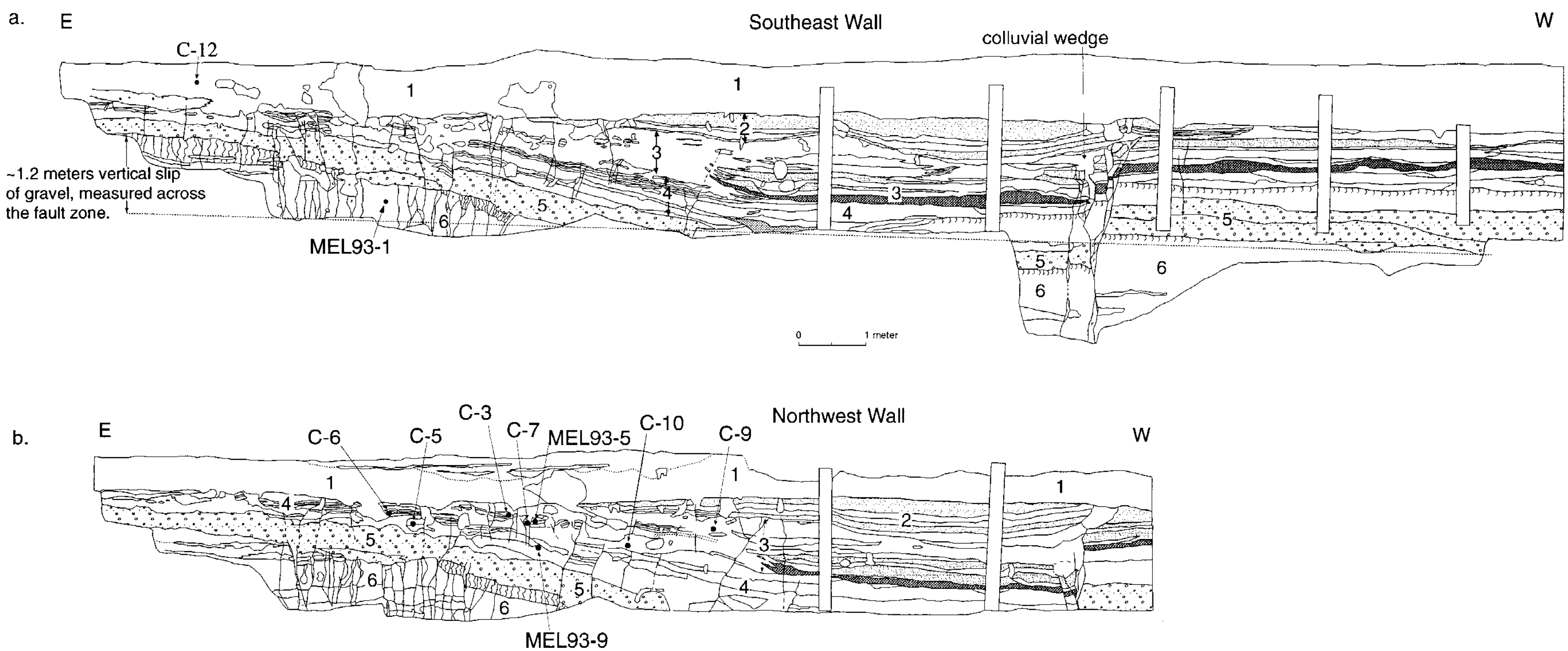

Figure 9. Log of the southeast wall of the Melville Gap trench.

Table 3
Radiocarbon Dates for the Melville Gap Site

Stratigraphic Unit	Sample Number	Laboratory Number	^{14}C Age (^{13}C corrected) B.P.	Calibrated Age B.P. (2σ)
1	C-12	Beta-62443/CAMS-6888	1680 ± 70	$1553^{+148}/_{-169}$
3	C-9	Beta-62444/CAMS-6759	8240 ± 70	$9258^{+212}/_{-229}$
3	C-10	Beta-62447/CAMS-6891	8170 ± 110	$9117^{+355}/_{-401}$
3	C-3	Beta-62445/CAMS-6889	8420 ± 70	$9444^{+97}/_{-154}$
3	C-7	Beta-62446/CAMS-6890	8710 ± 70	$9821^{+116}/_{-287}$
4	C-6	Beta-62448/CAMS-6892	8520 ± 100	$9528^{+321}/_{-216}$
4	C-5	Beta-62449/CAMS-6893	8550 ± 90	$9535^{+329}/_{-112}$

All samples are single pieces of detrital charcoal, and all samples experienced standard acid and base wash pretreatment. Calib 3.1 used for calibration.

upper part of the bedded section can be no older than 5.8 ± 0.2 ka on the basis of the TL and PSL ages. Similarly, unit 4 can be no older than about 7.5 ± 0.5 ka. Because all of the detrital charcoal dates from this part of the section yielded older ages, and because of evidence cited already (Rubin *et al.,* 1998; Vaughan *et al.,* 1999), we infer that this charcoal must all be reworked or have significant inherited age. We therefore use the TL and PSL ages as most representative of the actual ages of the exposed stratigraphy. We are aware of the possibility that our luminescence ages could be minimum estimates because of uncorrected anomalous fading of the luminescence from the feldspars (Aitken, 1998; Lamothe and Auclair, 1999), but we think that our preheating protocols (e.g., Berger, 1995; Ollerhead *et al.,* 1994) will have minimized any such effect, especially with the multialiquot methods we used. It is highly unlikely that for Holocene-age samples outside of an active volcanic region, age underestimation by 30%–50% (difference between charcoal and luminescence ages) would be observed. Rather, it is likely that anomalous fading unremovable by preheating (of multialiquot samples) is a regional problem (e.g., Lamothe and Auclair, 1999) and not universal. Certainly feldspars from some regional deposits (sediments from northern California, Washington State, and British Columbia; loess from Alaska; sand dunes from eastern Mojave; reviewed by Berger, 1995) provide accurate luminescence ages using multialiquot methods. Nevertheless, we recognize that future luminescence dating in this study region could employ more refined methods to test for and to identify any putative age-underestimation effects from uncorrected anomalous fading. We think that the simplest interpretation here is that the charcoal ^{14}C dates do not represent the time of last burial of the charcoal.

Evidence for Surface Ruptures. Three lines of evidence are used to assess the occurrence of past surface ruptures: upward abrupt truncation of fault splays, folding and warping of layers with coincident erosion across the fold, and the formation of colluvial wedges at the main fault scarp. During the past 11 ka, we see evidence for two and possibly three surface-rupturing earthquakes at the Melville Gap site, which did not experience rupture during the 1992 Landers earthquake.

The youngest event (M1) breaks the entire section up through unit 3 at the main fault on the western side of the graben, where the section is vertically separated by about 0.5 m. A small colluvial wedge was generated off the scarp, as shown in Figure 9. On the eastern side of the graben, which is primarily expressed as a fold, all strata up through the top of unit 3 are folded, and many fractures and faults with small amounts of vertical separation displace the finely laminated strata of units 4 up through 3. We attribute most of this deformation to a large surface rupture that occurred after deposition of unit 3. We reconstructed the vertical separation across the main, western fault (Fig. 10(a)), assuming that the separation represents vertical slip here, and we are able to rematch virtually every stratigraphic unit to the base of the trench. There are slight mismatches, most notably on the lowest units which may record an additional event, but the match is sufficiently good to preclude a similar scarp-forming event on the western side of the graben for the entire period recorded by the exposed section.

A finely laminated section of clay interbedded with sand (unit 2) overlies unit 3 and the colluvial wedge associated with the most recent event. The clay, which represents very low-energy depositional conditions, occurs only in the area of the graben and pinches out both to the east and west (Fig. 9). We interpret deposition of this section in a trough within the fault zone as a direct result of the faulting event (M1). The low-energy environment was afforded by the trough, which was probably a linear closed depression along the rupture.

Assuming that the luminescence date of 5.8 ka for unit 3 closely matches the event horizon, an age of about 5.8 ± 0.3 ka is assigned to event M1. However, because the sample from which this age was obtained was recovered from an eolian sand slightly below the top of unit 3, thus postdating event M1, it is therefore probable that the actual age of M1 is slightly younger. Nevertheless, on the basis of the relatively low sedimentation rate determined from the TL and PSL ages of units 3 and 4, and recognizing that eolian deposits may accumulate very rapidly, the top of unit 3 is prob-

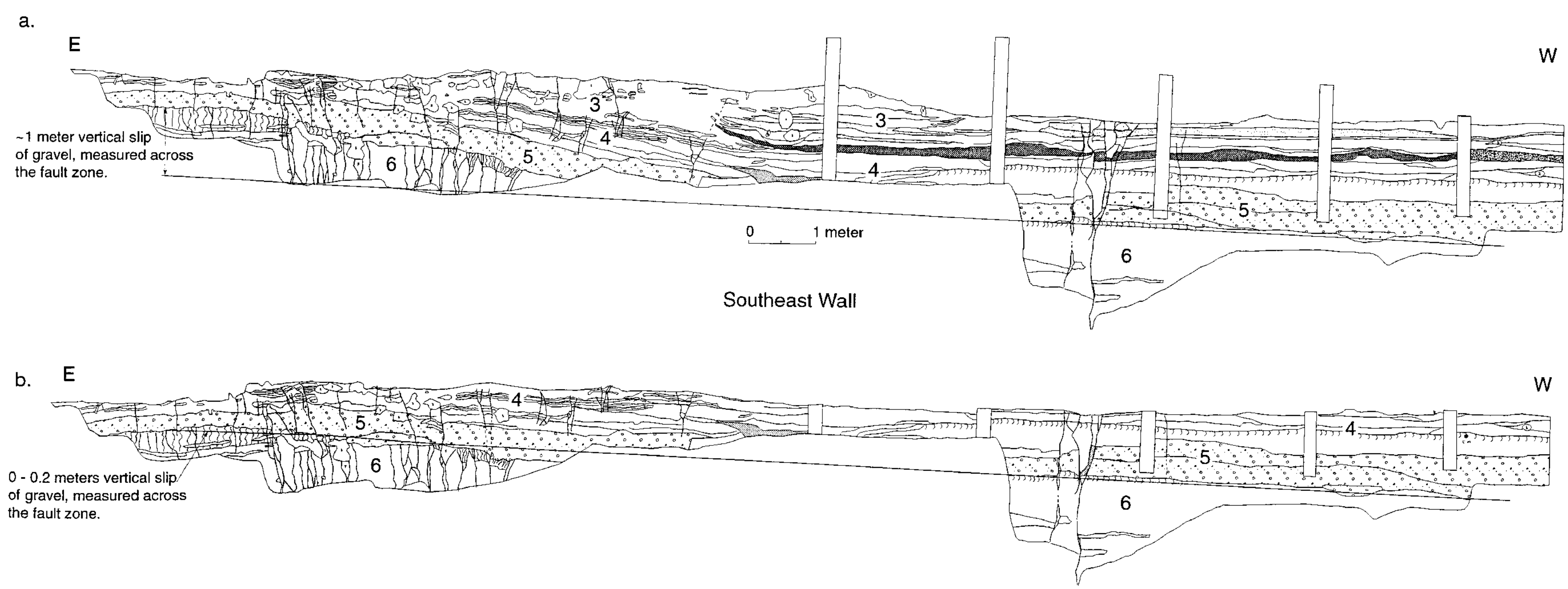

Figure 10. Reconstructions of the Melville gap trench log. (a) Removal of vertical separation of event M1. Note that unit 3 pinches out against the scarp to the east whereas unit 4 maintains constant thickness. (b) Reconstruction of units 4–6 to inferred configuration prior to event M2.

ably no more than a few hundred years younger than where we collected the sample. In the unlikely event that the TL and PSL dates are in error and the charcoal dates are valid, then this event actually occurred at about 9 ka.

An earlier event is indicated by folding and minor faulting on the eastern side of the graben that involves strata up through unit 4. Several faults with minor displacements break up through unit 4 and do not crack the overlying stratigraphy. Even though the vertical separations are generally less than a centimeter, the finely bedded strata allow for recognition of this event horizon based on upward termination of these minor faults. More compelling evidence for this penultimate event (M2) is found in the pattern of sedimentation before and after deposition of unit 4, which reflects folding of unit 4. Units 4 and 5 are of uniform thickness across the fold on the eastern side of the graben, indicating an equal amount of deformation. However, all overlying fine-grained units thin and pinch out across this fold, suggesting that a fold event occurred after deposition of unit 4. Based on this observation, taken with the minor faults that break unit 4 and not the overlying section, we infer that a displacement event occurred between deposition of units 4 and 3. There is no evidence that this event activated the western side of the graben, as the reconstruction in Figure 10(a) shows. Thus, this was either a smaller event or it concentrated slip on the eastern side of the graben. Because M2 produced greater overall east-side-up separation than did the most recent event (M1), it is likely that they were both relatively large events.

Finally, a third event is suggested by the presence of abundant fractures and minor faults that displace unit 6 but do not appear to penetrate into the base of unit 5 (Figs. 9 and 10). Unit 6 is also the only stratum that could not be realigned in the reconstructions of Figure 10, although that could also be due to lateral slip. Unit 5 maintains a fairly constant thickness across the fold, suggesting little or no folding deformation with this event. In that this is the coarsest unit in the section and obviously scoured locally into unit 6, it is possible that any fold that was present was simply scoured flat. Formation of a scarp along the western side of the graben could also have been scoured flat.

Alternatively, it is also possible that the fractures postdate deposition of unit 5 and their minor displacements were simply absorbed by the coarse, gravelly alluvium of this unit. Some fractures do break unit 5 and have fissures filled with unit 5 material (gravelly) penetrating downward into unit 6. Even some of these could not be shown to break the top of unit 5. Thus, although we maintain that an event is possible at this stratigraphic horizon, the overall evidence for this event is weak. If real, event M3 was probably smaller than either of the later two events based on the lack of folding and scarp formation.

The timing of events M2 and M3 are less well constrained than event M1. Event M2 occurred after deposition of unit 4. We TL-dated the base of unit 4 at 7.5 ± 0.5 ka and unit 3 at 5.8 ± 0.3 ka, bracketing the event horizon of event M2. In that the event horizon is only about 10 cm above the position of the TL sample that was collected near the base of unit 4, we infer that this event occurred soon after 7.5 ka. However, absolute constraints for this event are bound by the two aforementioned dates.

The event horizon for event M3 is at the top of unit 6, which is dated at 11.2 ± 0.7 ka. In that unit 6 may have been present for some time prior to the inferred event, this fracturing event may have occurred anytime between 11.2 ± 0.7 ka and 7.5 ± 0.5 ka, the age of overlying unit 4. If the charcoal dates are correct, which we consider less likely, then all three of these events occurred in a very short period of time about 9 ka ago.

In summary, we present evidence for two and possibly three surface ruptures along the northern segment of the Johnson Valley fault (that did not rupture in 1992) during the past 12 ka or so. Only the most recent rupture produced pervasive deformation throughout the width of the fault zone graben. Event M2 produced cracking and major folding and was almost certainly a significant earthquake. The interpretation of the occurrence of event M3 is arguable. If it did occur, then it was apparently a minor event or possibly triggered slip. Thus, there appear to have been two major and possibly one minor surface ruptures at the Melville Gap site in the past 12 ka or so.

We suggest that the earliest of the events (M3) at Melville Gap may have been a triggered slip event resulting from rupture on a nearby fault. Minor triggered slip occurred along portions of the northern Johnson Valley fault during the 1992 earthquake (Hart *et al.,* 1993). Specifically, a few mm of slip was observed at Bessemer Mine Road, a few km north of our trench site. Up to 5 cm of triggered slip was also recorded at Soggy Lake Playa on the Lenwood fault, and some of the observed minor slip along faults north of the main rupture may have been triggered slip and not primary rupture. Thus, it appears that at least in 1992, the main rupture was accompanied by triggered slip on nearby faults.

Alternatively, event M3 may represent a smaller earthquake, similar to the 1975 Galway Lake event or the 1979 Homestead Valley earthquake. Both of these earthquakes were only in the M 5.5 range and both produced minor surface rupture. If either of these interpretations are correct, then only two large surface ruptures have occurred along the northern Johnson Valley fault during the past 12 ka.

Homestead Valley Fault

Seven trenches were excavated at two sites along the Homestead Valley fault after the 1992 rupture, herein named the Thrust site and the Playa site (Fig. 1). The Thrust-site trench data and interpretations are presented as part of this article, being a principal component of our work after the earthquake. The Playa site was investigated by Hecker *et al.* (1993) and Cinti *et al.* (1993), and paleoseismic data and interpretations for the five trenches in their study are summarized for discussion purposes.

The Thrust-site trenches were the first two trenches excavated along the rupture after the earthquake. Figure 11(a) shows the complexity of the rupture through the area of study. Here, the fault makes a left jog, producing uplift and thrusting along with the strike-slip deformation. To the north and south of the Thrust site, cumulative strike slip from 1992 was measured at 3–4 m across a fairly narrow rupture zone (Sieh *et al.,* 1993). In the area of our trenches, only 1.2 m of strike slip occurred along the principal strand of the fault, with the balance of strain accommodated by distributed deformation and a thrust fault along the northern margin of the uplift. The thrust fault exhibited about 30–50 cm of vertical separation and essentially no horizontal slip; we measured 0 ± 5 cm of lateral slip on offset tire tracks at this site. Thus, we chose the Thrust site because there was clear evidence of only thrust displacement, which should be obvious in two-dimensional trenches across the fault. Furthermore, there are no assumptions about vertical-to-horizontal slip ratios and whether they have remained constant over multiple earthquake cycles.

The downside to the Thrust site is that the thrust fault, although a principal strand of the 1992 rupture in this area, is secondary to the main strike-slip fault. We must assume that all major ruptures have caused displacement on this fault and that the record for large surface ruptures is complete. As discussed later, this may not be the case. Nevertheless, we argue that large, 3–4 m slip events on the Homestead Valley fault should produce slip on the thrust, and there is clear evidence of repeated, similar-sized displacements in our trench. Smaller displacements on the Homestead Valley fault, however, may not produce rupture of the secondary structures, such as this thrust fault.

We excavated the two trenches along the thrust rupture about 20 m apart (Figs. 11(a) and 11(b)) because the expression of the surface rupture varied markedly from a 2-m-wide zone of shattering at trench site T-1 to an abrupt, simple scarp at trench site T-2. As discussed later, this resulted from a local change in subsurface stratigraphy that was not discernable from the surface geomorphology.

Trench T-1 exposed stratified, gravelly alluvial fan deposits (units 4 through 8 on (Figure 12(a)) capped by a discrete, 8-cm-thick buried A horizon (unit 3) that is interpreted to be principally of eolian derivation. These strata are overlain by about 0.5 m of slightly gravelly, medium-grained sand (unit 2) largely derived from an eroding dune complex upslope from the trenches. A 2-cm-thick eolian-derived vesicular A horizon (unit 1) caps the exposed section.

We described the soils in this trench to aid in the determination of deposit ages. The upper 0.5 m of alluvium has no B horizon but exhibits a stage I calcic horizon with thin, secondary $CaCO_3$ coatings on the undersides of the clasts. The minor accumulation of carbonate and the lack of a cambic B horizon is typical of late Holocene soils in the western Mojave region (Machette, 1985; Reheis *et al.,* 1989, Herzberg, 1996), so we infer a late Holocene age for this deposit.

The buried soil of units 3 through 5 exhibits a weak, ~10-cm-thick cambic B horizon with a slight increase in fines and very few secondary clay stains on grains (Table 1). A stage I calcic horizon is also present as coatings on clast undersides. Although slightly better developed than the overlying surface profile, comparison of this soil to dated soils in the Mojave region also indicate a Holocene age for these deposits, with a best estimate of 3–7 ka of surface exposure time (Reheis *et al.,* 1989) (Tables 1 and 4). Collectively, these observations and interpretations suggest that the entire section exposed in trench T-1 is Holocene in age and probably does not exceed 7–8 ka. None of the exposed strata appeared promising for TL dating, the sediments yielded no datable carbon, and we have no other data to constrain the age of the exposed deposits.

Faulting in trench T-1 occurred on a single, very narrow shear (~1 cm thick) that dips 28° to the southwest toward the main strike-slip fault (Fig. 12(a)). As the fault approaches the surface, it gradually rolls to a 22° dip at 50-cm depth, where it abruptly flattens to a nearly horizontal attitude. This gradual rolling over of the fault as it approaches the surface resulted in minor extension in the hanging wall, expressed as many cracks and fissures that extend to a depth of 50–70 cm. It appears, however, that all of the actual slip occurred on the primary rupture surface.

Reconstruction of the scarp produced by the 1992 slip realigns all of the stratigraphic units and their contacts (Fig. 12(b)) and demonstrates that about 85 cm of dip slip occurred on the thrust at this location. The reconstruction also shows that there is no evidence for a previous rupture of the strata exposed in trench T-1. Using the soil ages estimated earlier, there does not appear to be any other middle to late Holocene ruptures along this thrust.

Trench T-2 exposed a very different sequence of strata, with only the capping eolian A horizon in common with the strata of trench T-1 (Fig. 13(a)). This was initially surprising because there is very little surface geomorphology to suggest such a difference in subsurface stratigraphy (Fig. 11(b)). The strata of trench T-2 contain two buried soils, both of them with substantially better development than either soil exposed in trench T-1, indicating a much longer stratigraphic record. The stage III calcic horizon of unit 8 in and of itself indicates a minimum surface exposure time of many tens of thousands of years, as discussed later. Apparently, trench T-1 was excavated in a swale or buried channel that backfilled during the Holocene. This buried channel apparently incised strata of trench T-2, interpreted to be largely Pleistocene in age based on the strength of their soil profiles and a single TL date on unit 4 (~15 ka; Table 2).

The surface soil, developed through units 2 and 3, is very similar to the soils exposed in trench T-1 (Table 1). Although lacking a Bw horizon, there is a stage I calcic horizon and consequent moderate development of soil structure. Due to the lack of a Bw horizon, and the shallow depth at which the carbonate accumulated, we interpret these deposits to be late Holocene in age.

A buried soil is developed through units 4–7 on the footwall of the fault. Unit 4 is a wedge-shaped pebbly sand deposit that thickens abruptly at the fault, and thins northward to zero at the northeast end of the trench. This deposit is interpreted as a colluvial wedge shed off of the fault. A cambic Bk horizon is developed in the lower portion of unit 4 and extends downward into unit 5, a massive to slightly stratified gravelly sand. This Bwk horizon, which is 35-cm thick, has common clay stains and a few clay films, moderately developed structure, and stage I+ calcic development. The color, carbonate, and clay drop off downward into the C horizon with minimal secondary carbonate in units 6 and 7. Unit 8 on the footwall is capped by another buried soil that expresses an argillic horizon and a superposed stage II+ calcic horizon (Table 1).

The calcium carbonate accumulation in both the Bwk horizon of unit 5 and the Btk horizon of unit 8 are interpreted to be, at least in part, the result of secondary overprinting by their respective overlying deposits and soils. It is unlikely that both carbonate and clay accumulated simultaneously in unit 8. Rather, the carbonate of unit 8 is interpreted to be the primary calcic horizon of the soil associated with units 4–7. This is supported by the presence of carbonate pipes extending upward from the top of unit 8 into unit 7, indicating that most or all of the carbonate came from flushing of the overlying units. Similarly, we interpret part of the carbonate accumulated in units 4 and 5 to be associated with the soil development of units 2 and 3. If this interpretation is correct, then the soil developed through units 4–7, in addition to the 35-cm-thick Bw horizon, has a stage II+ calcic horizon associated with it.

This interpretation is preferred for several reasons. First, Holocene cambic horizons described in the Mojave and Imperial Valleys of southern California rarely exceed about 10 cm in thickness, similar to all those described in this study. B horizons with thicknesses of 30–50 cm are almost exclusively associated with Pleistocene deposits which developed during periods of higher precipitation. Their calcic horizons are also correspondingly deeper. For some of the soils described in this study, such as in the Hondo site trench, the Pleistocene soil exhibits a moderately developed argillic horizon and no calcic horizon, indicating sufficient moisture during the Pleistocene in that area to flush the profile. At the Thrust site, the obvious accumulation of significant calcium carbonate indicates that Homestead Valley was drier during the late Pleistocene than farther west, near the San Bernardino Mountains range front. Nevertheless, based on the thickness of the Bwk horizon, the calcic carbonate should accumulate at greater depth. We suggest that the presence of the buried argillic horizon of unit 8, with much higher moisture retention than the overlying deposits of units 5–7, forced deposition of $CaCO_3$ associated with the soil of units 4–7, hereafter referred to as buried soil 1.

Comparison of buried soil 1 with those in the western Mojave Desert suggests a late Pleistocene age with 12–35 ka in surface exposure time. Similarly, the buried argillic horizon of unit 8, although not completely exposed, must represent a longer period of exposure. A similar-appearing argillic horizon at the Hondo site trench (unit 6) is dated at about 50 ka (Tables 1 and 2). We tentatively place a similar surface exposure time for unit 8 in the footwall of Trench T-2. Thus, the depositional age of unit 8 must be the cumulative age of both buried soils, or about 60–100 ka.

The soils developed in the hanging wall deposits are somewhat simpler to interpret. Units 2 and 3, which contain the weakly expressed late Holocene soil, overlie an argillic horizon (unit 8) and an associated K horizon with stage III carbonate development (unit 9). Stage III calcic horizons in the Mojave region are estimated to require at least 50–100 ka to develop (Machette, 1985; Reheis *et al.,* 1989). Thus, we place a tentative minimum age of 50–100 ka for the hanging wall deposits in trench T-2.

The fault exposed in T-2 maintains a fairly constant dip of about 15° probably due to the competence of the sediments. At the surface, the snout at the fault tip collapsed, producing a pile of rubble (unit 1) along the rupture trace (Fig. 13(a)). We reconstructed the 1992 slip by unslipping along the fault, realigning units 2 and 3, and attempting to remove the scarp (Fig. 13(b)). We were unable to completely remove the scarp with our reconstructions and a slight bow is still present. We interpret this to represent the presence of a degraded scarp at this site prior to the 1992 rupture.

The 1992 slip determined from this trench (about 85 cm) is identical to that reconstructed in trench T-1. Because both observations were the same, we use 85 cm as the minimum amount of slip accommodated by the thrust in this area. An additional thrust fault trace, with a scarp height of about 10 cm, is present south of our trenches and also accommodated some 1992 slip. If the fault dips are similar, then an additional 15–20 cm of thrust displacement also occurred on the southern strand. Thus, cumulative thrust displacement at our site was about 1 m in 1992, with most (85 cm) occurring on the northern trace.

Evidence for Prior Surface Ruptures in T-2. There is structural and stratigraphic evidence for multiple slip events exposed in trench T-2. An older fault strand is present above the 1992 rupture surface that breaks up to unit 4 but does not displace its lower and upper contact (Fig. 13). The fault appeared to crack unit 4, but there was no displacement, and the cracking may be attributed to 1992 shaking. Unit 4 itself is a very localized deposit that is thickest at the fault and thins to zero at the northern end of the trench. Furthermore, once the 1992 slip is removed (Fig. 13(b)), the Pleistocene surface soils associated with the top of units 8 and 4 exhibit a rounded scarp buried by unit 4. We interpret all of these factors as evidence for a previous event that ruptured when units 8 and 5 were at the surface. We also interpret unit 4 as a colluvial wedge shed off of the scarp produced by this penultimate event. The buried scarp and colluvial wedge have been subsequently buried by the Holocene deposits of units 2 and 3, which had removed most of the geomorphic evidence prior to the 1992 event.

We collected a TL sample from the colluvial material

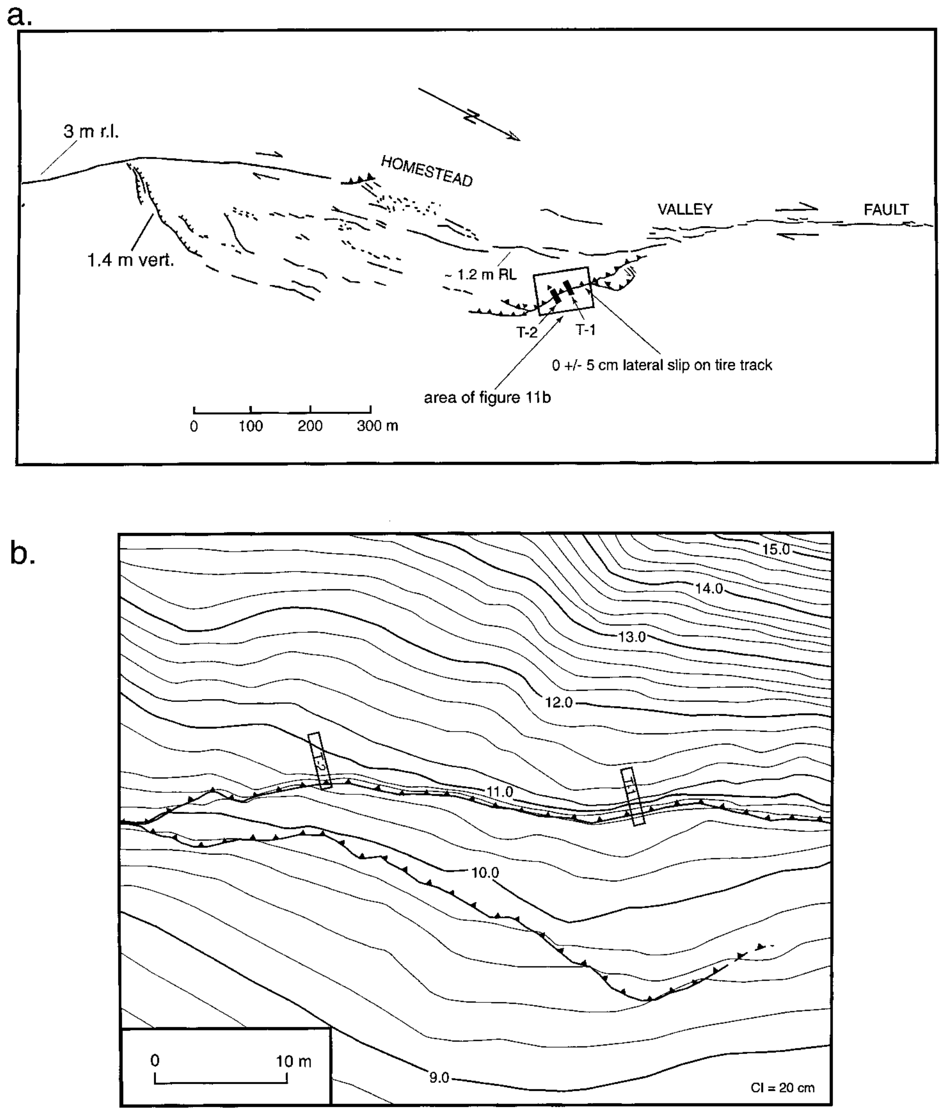

Figure 11. (a) Map of the rupture in the vicinity of the Thrust site. Note that our trenches are on secondary thrust faults and not the primary rupture. (b) Topographic map of the thrust ruptures at the Thrust site. Contour interval is 15 cm.

of unit 4. The resulting corrected age of 15.0 ± 1.1 ka (assuming a similar relict age as at the Hondo site) indicates that the penultimate thrust displacement at this site occurred at about 13–17 ka, during the late Pleistocene.

A late Pleistocene age for the penultimate event is consistent with our soil age estimates (12–35 ka). Although the Bw horizon developed in unit 5 extends up into unit 4, the majority of secondary clay is in unit 5. This suggests that a substantial portion of the soils development occurred prior to deposition of unit 4, which was produced by the penultimate event. A late Pleistocene age for the event would be consistent with this and allow for some continued soil development in unit 4 after accumulation of that colluvium.

We also reconstructed the slip produced in the penultimate event, to assess its amount of dip slip, by realigning the tops of units 5 and 8, the two Pleistocene buried soils (Fig. 13(c)). This required an additional 80 cm of backslippage, indicating that the penultimate earthquake produced a nearly identical amount of slip as occurred in 1992 at this site.

With the reconstruction of the past two events, it is clear that unit 5 must have been present prior to the prepenultimate event because unit 8 is thrust over unit 5. Using our 12–35 ka age estimate for the soil developed through unit 5, this suggests that the two events prior to 1992 occurred during the past 35 ka, or less.

Finally, we also estimate that about 4.5 m is required to reconstruct unit 8, which is estimated to be 50–100 ka in age. This is roughly 5–6 times the amount of slip that occurred in each of the past two events. If the 1992 slip is representative of most displacements on this fault, then these data suggest an average long-term recurrence interval of

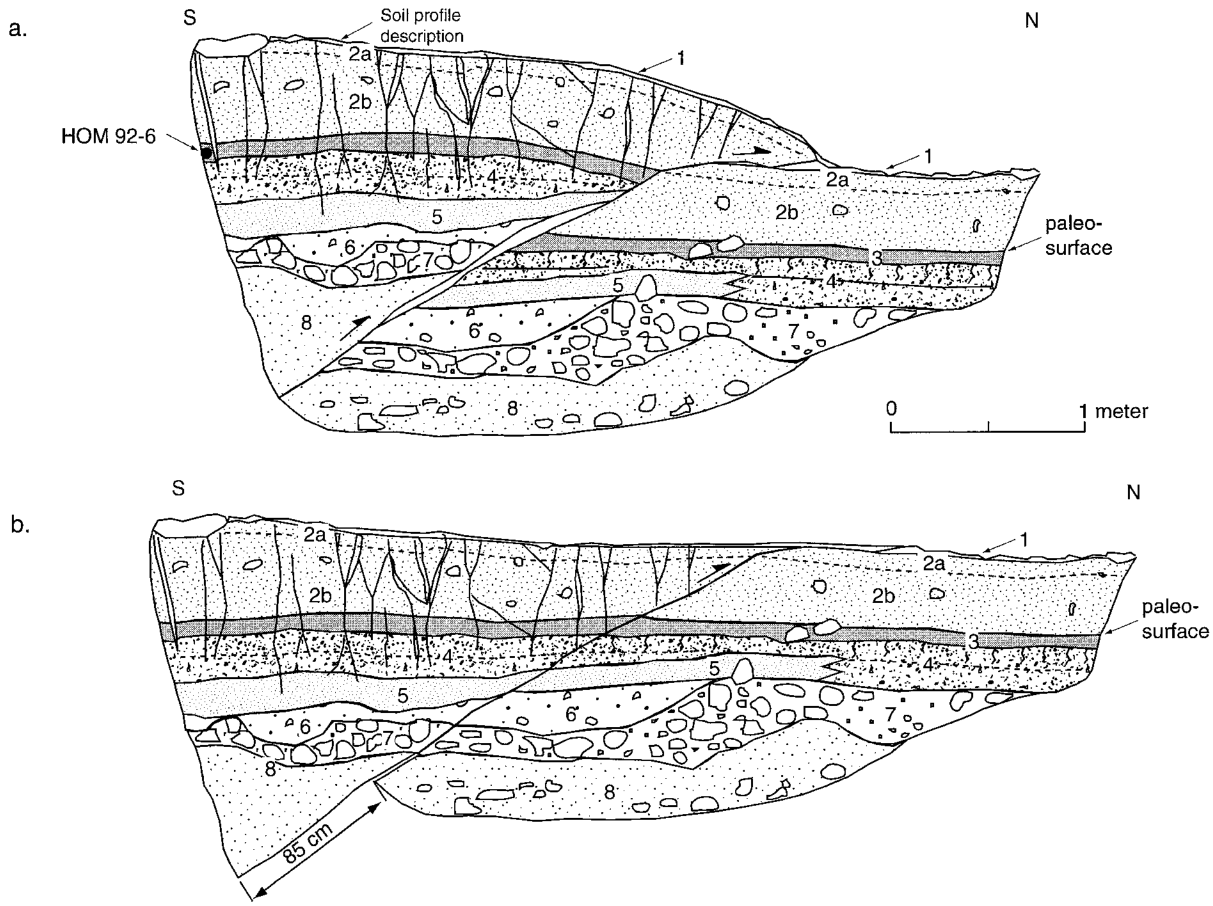

Figure 12. Log of trench Thrust T-1. (a) Log of T-1 after the 1992 earthquake; (b) reconstruction of the ground surface to pre-1992 configuration. In that there was no strike slip at this site, there are no concerns about slip versus separation. Note that the reconstructed section is balanced and requires only the 1992 surface rupture.

about 8–20 ka (5–6 events divided into 50–100 ka). This is consistent with the TL date on the colluvial wedge, placing the penultimate event at about 15 ka.

Playa Site Summary

Five trenches were excavated by Hecker *et al.* (1993) across the Homestead Valley fault at a playa, located about 3 km northwest from our Thrust site. Here, fluvial and distal alluvial fan sediments have accumulated against a low scarp along the primary strand of the Homestead Valley fault (Cinti *et al.,* 1993; Hecker *et al.,* 1993) (Figs. 1 and 8). The 1992 slip in this area was about 3 m of dextral slip and 0.4 m of localized dip slip (Hecker *et al.,* 1993; Sieh *et al.,* 1993). The vertical component of slip, along with the evidence of prior vertical displacements, made this site attractive for paleoseismic study.

Hecker *et al.* (1993) document evidence for up to three paleoseismic events, based on stratigraphic and structural relations exposed in their trenches. Using both ^{14}C dating on detrital charcoal and TL dating on the finer-grained alluvial elements, they date the penultimate surface rupture (P2) to between 5.7 and 8.5 ka. They also date the prepenultimate event (P3) as having occurred shortly before 12.5–14 ka. The size of the penultimate event is inferred to be similar to that of 1999, at least at this site, based on comparisons between the amount of vertical separation in 1992 with that expressed in this earlier event, about 35 cm.

There is not a good correlation of events between the Thrust and Playa sites. In fact, at the Thrust site, we see no evidence for their penultimate event (P2) between 5.7 and 8.5 ka, although their P3 event may correspond to our penultimate event (T2). There are three plausible explanations for these observations. First, the Thrust site simply does not record every large Homestead Valley earthquake. If this is the case, then the Playa site record is more complete and provides evidence for additional prehistorical events.

Another possibility is that the penultimate event at the Thrust site is actually much younger than that inferred from the TL and soils data. The TL date is a maximum age for the colluvial wedge, and if the wedge material had as much as 9 ka of relict age, then this interpretation is plausible. The problem is that we see no evidence from any of the TL results

Table 4
Results from Trenching Sites on Southwestern Mojave Faults

	Fault Segment	Site	Timing of Major Surface Ruptures (+/− 1σ)(ka)	Estimated Average RL Slip (m)	Slip Estimate Method*	Estimated Rupture Length (km) (assumes entire segment ruptures)	Seismic Moment (10^{27} dyne cm) (assumes 13.5 km depth)	Estimated Moment Magnitude (M_w)	Sum of fault strands involved in 1992 rupture (M_o and M_w)
1	S. Johnson Valley	Hondo	1992, 4.7 ± 0.7, 10 ± 2	3	a	24	3.0132E + 26	6.9	
	S/N Johnson Valley	Batdorf	1992, 9 ± 2.6, 18.5 ± 1.6						
2	Kickapoo	Bodick Rd.	1992, 5.3 ± 0.5	3	a	included w/ sJVF			1.29526E + 27
4	Homestead Valley	Thrust	1992, 15 ± 1.1	3	a	30	3.7665E + 26	6.9	7.3
	Homestead Valley	Piaya	1992, 7.1 ± 1.4, 14 ± 1.5	0.65	c	30	8.16075E + 25	6.5	
6	N. Emerson	Piaya	1992, 8.7 ± 0.2, 19.5 ± 4.5	4	a	32	5.3568E + 26	7	
7	Camp Rock	Graben	1992, 1 ± 1, 9.5 ± 1, 14 ± 3	1.4	a, c	35	2.05065E + 26	6.8	
8	S. Homestead Valley	Landfill		0.25	c	10	1.04625E + 25	5.9	
9	N. Johnson Valley	Melville Gap	5.8 ± 0.3, 7.5 ± 1.5, 9.3 ± 2	0.8	c	36	1.20528E + 26	6.6	
10	Lenwood	Soggy Lake	<1.3, 5.6±1, 8.9 ± 1	3	b	75	9.41625E + 26	7.2	
11	Old Woman Springs	OW Spring	0.3 ± 0.1	3	c	included w/ Lenwood			
12	Helendale	Rabbit Springs, Waverly	1.1 ± 1, 9 ± 2,	1.45	c	62	3.76232E + 26	6.9	
13	Hector Mine EQ	1999 rupture	1999, 30–50 ka	3	a	35	4.39425E + 26	7	

Used 5.0 ± 0.9 ka for the penultimate sJVF and KF rupture by combining paleoseismic data from both faults.

Used 15.0 ± 1 ka for the penultimate large HVF rupture by combining paleoseismic data from both the Thrust and Playa sites, assumed smaller for penultimate event.

Used 10 ± 2 ka for sJVF prepenultimate rupture based on paleoseismic data at Hondo and Batdorf.

*(a) Assumed 1992 and 1999 slip is representative for this segment; (b) Slip based on field geomorphic measurements (Padgett and Rockwell; 1994); (c) Slip estimate based on rupture of entire segment and average slip/rupture length relationships of Wells and Coppersmith (1994); (a,c) Estimated average slip is the mean between methods a and c.

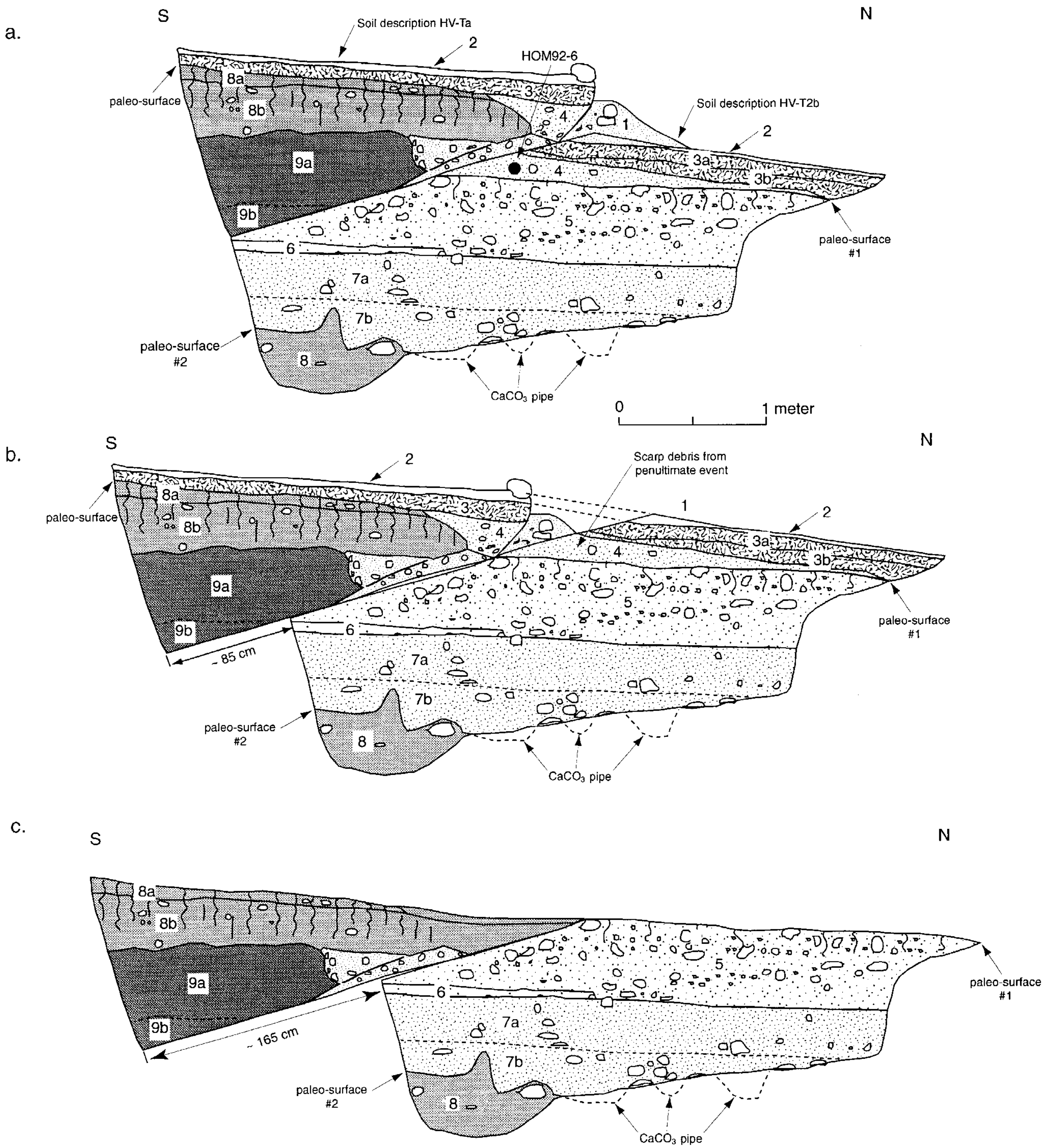

Figure 13. Log of trench Thrust T-2. (a) Log of T-1 after the 1992 earthquake. (b) Reconstruction of the ground surface to pre-1992 configuration. In that there was no strike slip at this site, there are no concerns about slip versus separation. (c) Reconstruction of the penultimate event, which demonstrates that dip slip was similar to 1992, about 85 cm.

from our Landers studies that would corroborate this magnitude of an inherited age. Further, there is clear evidence of translocated clay in the wedge that occurred after its deposition, indicating a substantial period of surface exposure prior to burial by the middle to late Holocene deposits. Although the component of soil development in the colluvial wedge (unit 4) is plausibly as young as middle Holocene in age, we consider it unlikely.

The third possibility is that the penultimate paleoseismic event at the Playa site was smaller than inferred from its vertical separation and this event was not large enough to activate the secondary thrust fault at our site. This, of course, assumes that all large slip events (3–4 m) along the Homestead Valley fault will cause activation of the thrust fault at the Thrust site and that smaller events will not. In this scenario, the record at the Thrust site is also incomplete, but largely due to the Thrust site's inability to record smaller events.

A variant of the third scenario is that rupture propagation direction plays a role in whether or not the thrusts are activated. If the thrusts move only during northward propagating ruptures, such as occurred in 1992, then the Thrust site record may be incomplete and not record some events that propagated from north to south. However, we see no structural or kinematic reason why activation of the thrusts would necessarily depend on rupture direction.

We favor the third scenario because the structural complexity of the Homestead Valley fault in the vicinity of the Thrust site does not allow for simple transfer of strain through the restraining bend. We consider it unlikely that other large, 3–4 m slip events would have maintained high slip along the primary fault, but rather have caused distributed deformation similar to that in 1992, which involved the thrust fault. This is supported by our observations of the narrowness of the thrust fault at shallow depths that indicate it has repeatedly broken during the late Quaternary in the same place. This also indicates that the restraining bend is not a new phenomenon along this portion of the fault zone.

Long-Term Temporal Pattern of Mojave Earthquakes

We compare our paleoseismic results from the southern Johnson Valley, Kickapoo, and Homestead Valley faults with those from other studies along the Homestead Valley fault (Hecker *et al.,* 1993; Cinti *et al.,* 1993), Emerson fault (Rubin and Sieh, 1997), and the Camp Rock fault (C. Rubin, written communication), all of which ruptured in the 1992 Landers sequence. In this comparison, we also included our paleoseismic data from the Northern Johnson Valley fault (Herzberg and Rockwell, 1993; this article) and available data from other faults in the ECSZ that were not involved in the 1992 event. These data included trenching studies on the Lenwood (Padgett and Rockwell, 1994), Old Woman Springs (Houser and Rockwell, 1996), and Helendale (Bryan and Rockwell, 1994) faults. A compilation of the timing of moderate to large surface-rupturing events, with their associated errors in age assessment, are presented in Figure 14 and Table 4.

In Figure 14, there appears to be clusters or groupings of past earthquakes centered around 0–1 ka, 5–6 ka, and 9–10 ka. Older groupings may also be present but data are too sparse to delineate these. Between these apparent clusters, large earthquake activity was apparently low for a period of several thousand years, and in the period between about 1.5 to 4.5 ka, we see no evidence for large earthquakes on any of the faults that we have thus far studied. In contrast, nearly all of the faults in the southwestern part of the ECSZ have ruptured during the past thousand years or so.

The groupings during the past ten thousand years are fairly robust although errors for some of these paleoevents are substantial. Furthermore, not all of the events are necessarily of the same magnitude, and some of the sites listed in Table 4 and shown on Figure 14 record the same event. To assess the temporal patterns of moment release for the faults that we have studied, we make an attempt at estimating the amount of moment produced by each of the events that we recognize in each of these trench studies. To calculate moment, we assume rupture of the entire mapped fault length and a seismogenic depth of 13.5 km, which is based on the centroid depth determined for the Hector Mine earthquake (Scientists from the USGS, SCEC, and CDMG, 2000). Multi-segment or multi-fault ruptures are thus accounted for because moment is summed on a fault by fault basis. To estimate average slip, we used information derived from either geomorphic studies of offset stream channels, 1992 slip measurements for faults involved in the Landers earthquake, or estimates derived from Wells and Coppersmith (1994) based on fault length.

For the Lenwood fault, there are direct data from detailed study of the geomorphology that provide estimates of the amount of slip per event (Padgett and Rockwell, 1994). In their study, they determined that the past several earthquakes each produced about 3 m of slip near Soggy Lake Playa, the site of the paleoseismic investigation, based on many small ephemeral drainages that cross and are interpreted to be offset by the Lenwood fault. Thus, we use 3 m as the average slip for large surface ruptures for that fault, consistent with its approximately 75 km length. We also assume that the Lenwood and Old Woman Springs faults are essentially a single fault, as they are part of the same fault zone separated by a restraining step-over and the timing of the most recent event is indistinguishable for each fault, within errors.

For faults that ruptured in the 1992 earthquake, we use the 1992 slip as an estimate of the average slip for that fault, at least for most events. The only exception is for the Homestead Valley event at about 7.1 $\pm$ 1.4 ka that we infer to be smaller based on its absence from our Thrust site trenches. In this case, and for all other faults where we have no direct information on slip per event, we take the mapped length of the fault and calculate average slip based on the published relationships of Wells and Coppersmith (1994) (Table 4).

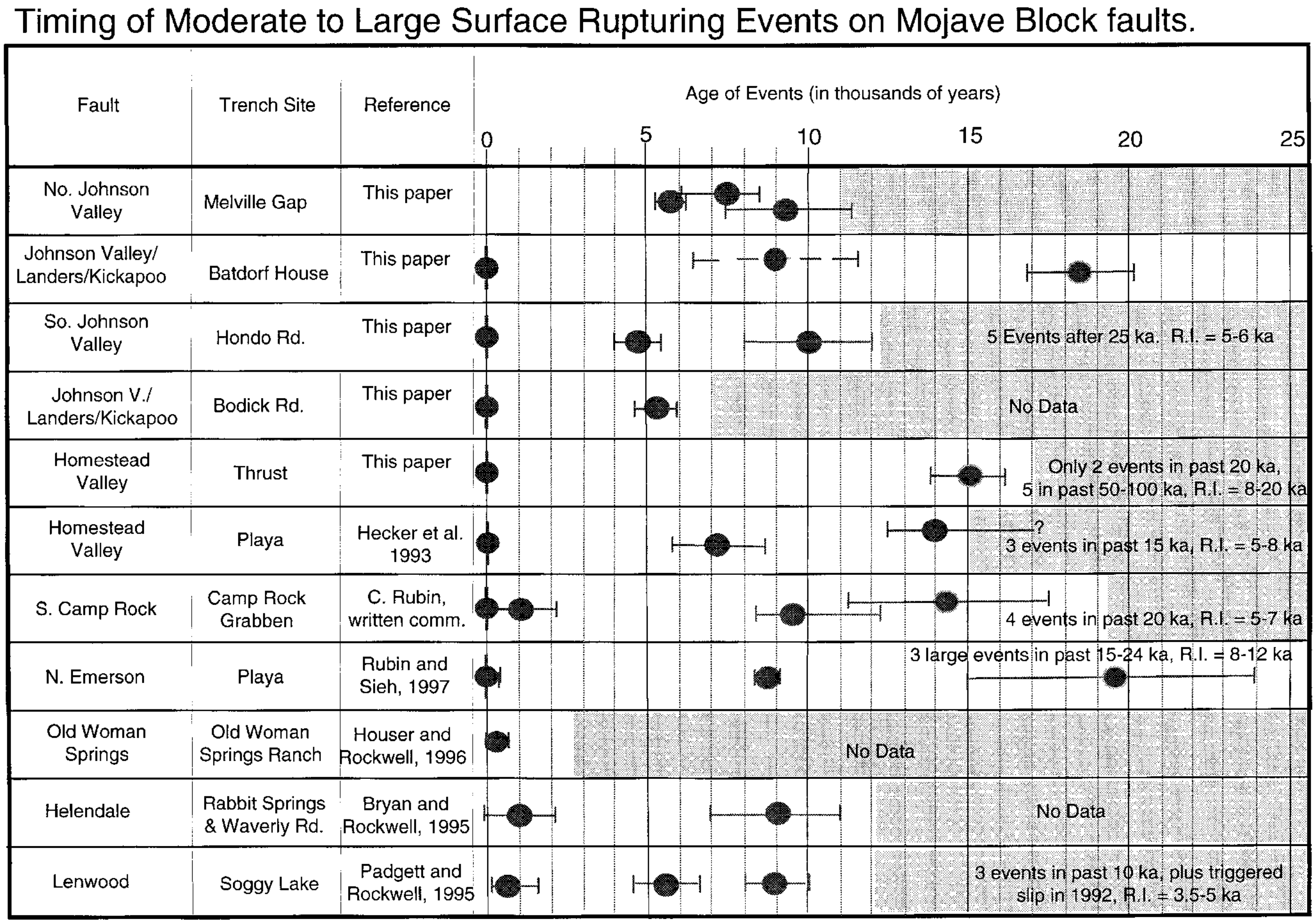

Figure 14. Diagram showing the timing of past earthquakes at all trench sites. Errors are shown as bars. Note that some earthquakes depicted at different sites are probably common events. Also note that data are lacking for older events (shaded areas) for many sites.

Moment release can be evaluated in several ways, and we have chosen a method that accounts for the inherent errors in dating prehistoric earthquakes, especially in arid regions where precise dates are rare. Figure 15 represents a series of moment release curves for individual faults involved in this analysis. The shape of each curve is a probability density function where the error in event dating is accounted for by the shape of the function, and the area under each curve scales to the moment of that event. Thus, poorly dated paleoearthquakes have broad curves that effectively distribute the released moment over a period of time whereas well-dated events have high curves narrowly centered on the date of the earthquake. Because the 1992 earthquake would be represented as a line of infinite height using this method, we arbitrarily assigned a $\pm$ 50 year error function for this known event to allow it to scale with the prehistoric events. The black curve represents the sum of all moment release from earthquakes that we have identified in our trenches and from the various other paleoseismic investigations.

Using this method, there is a distinct pattern of clustering that is fairly robust for at least the past three cycles. These correspond very well with those inferred from the more qualitative data of Figure 14, and argue for distinct periods or bursts of seismic activity punctuated by periods of relative quiescence. Individual faults, however, appear to behave in a quasiperiodic fashion, with the clustering produced by the in-phase earthquake generation of the system of faults.

It is not clear if this pattern is representative of the entire ECSZ or just the southwestern portion of the Mojave desert. It is possible that seismic activity migrates from one part of the shear zone to another over time scales of thousands of years and that there is a sampling bias in our data. It is also possible that this pattern represents a fundamental process in regional strain release, as noted by the "surprising large long-term temporal and spatial variations" in seismic activity in areas of long historical record (Allen, 1975). Further work will hopefully resolve the past seismic activity of other faults in the ECSZ and test whether clustering has affected the entire Mojave region.

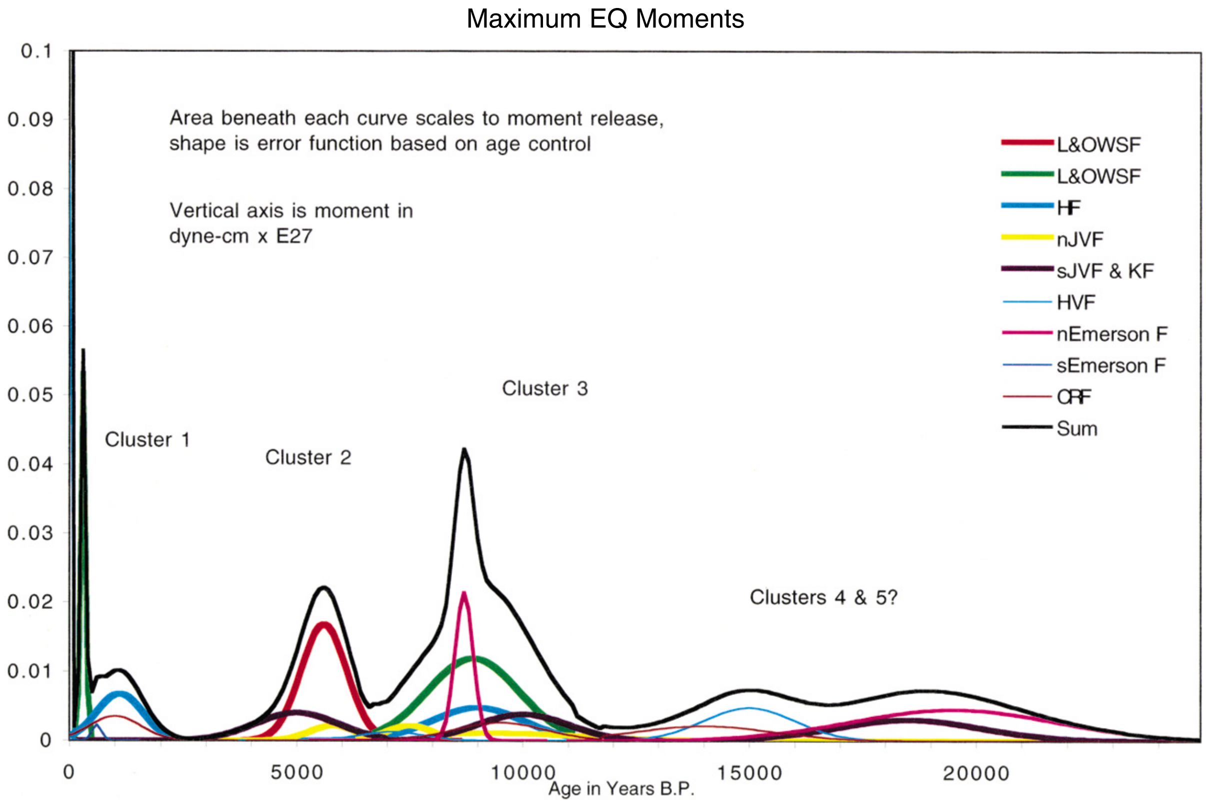

Figure 15. Moment release over time for western Mojave faults. Moment scales to the area under the curve, which are probability density functions that represent the error in age assessment of each event. The uppermost black curve (Sum) is the sum of moments for all events. L&OWSF, Lenwood and Old Woman Springs fault; HF, Helendale fault; nJVF, northern Johnson Valley fault; sJVF & KF, southern Johnson Valley and Kickapoo faults; HVF, Homestead Valley fault; nEmerson F and sEmerson F, the northern and southern Emerson faults, respectively; and CRF, Camp Rock Fault.

Discussion and Conclusions

We excavated 11 trenches at 7 sites along faults that ruptured in the 1992 Landers earthquake to establish the late Pleistocene and Holocene rupture history of each of these faults. Data for some faults is more complete than others, and ages of earthquakes are also better constrained at some sites than others. We use these new data, in conjunction with information collected by Rubin and Sieh (1997), Zachariasen and Sieh (1995), and Hecker *et al.* (1993) to test several ideas that were generated by this large, and largely unexpected, event.

Issue 1. Did the 1992 rupture proceed onto the Kickapoo and Homestead Valley faults because the northern Johnson Valley fault had recently failed? At the Melville Gap site, we have established that the northern portion of the Johnson Valley fault has not ruptured since about 5.8 ka or slightly thereafter. We can also demonstrate the occurrence of two large events (at about 5.8 and 7.5 ka) during the past 12 ka at the Melville Gap site, with one other, probably smaller, event at about 11.5 ka B.P. Thus, the average return time for large surface ruptures appears to be on the order of several thousand years, but not ten thousand years or longer. These observations counter the idea that the Landers rupture proceeded onto the Kickapoo fault rather than the northern Johnson Valley fault because it was insufficiently stressed to rupture in 1992. In fact, because it has been over 5 ka since the most recent event, we suggest that the northern Johnson Valley fault is a candidate for a near-future event.

In discussing whether rupture of the southern Johnson Valley fault may just as well have proceeded northward along the northern Johnson Valley fault, we suggest that rupture direction may have played a role. Further, it is possible that rupture direction, and possibly point of nucleation, influences extent of faulting during any given event cycle. The 1992 earthquake nucleated near the southern end of the Johnson Valley fault and propagated northward. The Kickapoo fault is nearly colinear with the southern portion of the Johnson Valley fault, so northward rupturing events may simply be favored up this pathway rather than toward the northwest, which requires the rupture to jog left through a restraining single bend (Fig. 1). In contrast, ruptures that begin in the north and propagate southward would view this bend as a releasing or extensional bend. Sowers *et al.* (1994)

noted that sinter mounds are present along the southernmost portion of the northern Johnson Valley fault, as well as just south of its intersection with the Kickapoo fault, indicating extensive hydrothermal flooding at some time in the past. These deposits may reflect hydrothermal activity that occurs after southward-directed rupture propagation, which should produce extension in the bend area. Releasing steps and bends commonly form the endpoints of strike-slip fault ruptures (Sibson, 1985; Knuepher, 1989) so southward rupturing events may terminate at the bend rather than continue south of the Kickapoo-Johnson Valley fault intersection. This may explain the additional Holocene event at the Melville Gap site at about 7.5 ka, which is not recognized on either the southern Johnson Valley or Kickapoo faults (unless E3 at the Hondo site is the same event as E2 at the Melville Gap site, which we consider unlikely although not implausible). A 30-km-long rupture of only the northern Johnson Valley fault would correspond to about a M_w 6.8 event, assuming Wells and Coppersmith (1994) relationships among rupture length, moment magnitude, and average slip. In any case, considering the length of time since the most recent event at Melville Gap, it is fair to conclude that the 1992 rupture path was not substantially influenced by a recent past event.

At the juncture of the Johnson Valley and Kickapoo faults, we see evidence for only two pre-1992 surface ruptures during the past 20 ka, which probably reflects the rupture history of the Kickapoo fault. At the Bodick site on the Kickapoo fault, we date the penultimate event to 5.3 ± 0.5 ka, indistinguishable from the northern and southern Johnson Valley faults, and the prepenultimate event as late Pleistocene, consistent with the Batdorf site data. Thus, it appears that the Kickapoo fault and the northern and southern Johnson Valley faults may all have failed together in the penultimate event, or failed as a cluster over a short time interval. Prior to that event(s), they appear to have had independent slip histories, at least during the late Quaternary.

Issue 2. Was there evidence for the occurrence of similar earthquakes in the past and could we have forecast the likelihood of these five faults failing together in one large, complex event? Another primary issue that we addressed was whether there have been past events similar to the 1992 event, and whether we could have forecast the likelihood that the 1992 earthquake would be as large as it was. The latter issue is easier to address. The timing of the penultimate event on the southern Johnson Valley and Kickapoo faults are indistinguishable at close to 5 ka, so they could have been the same event. However, it appears that the Emerson fault failed substantially earlier, at about 8.7 ka (Rubin and Sieh, 1997), and was not involved with the penultimate Johnson Valley event. The penultimate Homestead Valley event (Hecker *et al.,* 1993) is permissibly the same as the penultimate Johnson Valley and Kickapoo events, although the age data suggest that it may have been as much as a thousand years earlier. Furthermore, based on our Thrust site data on the Homestead Valley fault, we argue that the event P2 recognized by Hecker *et al.* is smaller than that which occurred in 1992. These observations indicate that the 1992 surface rupture was not simply a repeat event. Thus, without the hindsight provided by the 1992 event, it is doubtful that anyone would have proposed the magnitude, rupture pattern, or amount of displacement.

However, there are earlier candidate earthquakes that may have been similar to the 1992 event, and the most plausible candidate occurred at about 15 ka. We argue that the last large surface rupture along the Homestead Valley fault occurred about that time, based on activation of the thrust fault at the Thrust site. Although Hecker *et al.* (1993) report evidence for another surface rupture after 15 ka and prior to 1992, we suggest that it may have been smaller than the 3 m that occurred in 1992. This inference is based on the idea that only large displacements, similar to 1992, will activate the secondary thrust fault whereas smaller slip events will bypass it.

Rubin and Sieh (1997) documented that the Emerson fault slipped between about 15 and 24 ka. However, their radiocarbon dates were on pedogenic carbonate which has inherent residency problems (Gile *et al.,* 1981). Thus, it is possible that the penultimate Emerson event was younger, at about 15 ka, than the mean age suggested by Rubin and Sieh (1997), in which case it may have been involved with a Landers-type earthquake. Nevertheless, taken at face value, that Emerson event was likely older than the 15 ka date inferred for the last large Homestead Valley event, and thus, there may be no other event similar in size and extent to 1992 for the past 20 ka or so. Consequently, it is unlikely that if we had completed all of our trenching prior to 1992, that we would have recognized the potential for all five faults failing in one earthquake sequence.

Issue 3. Do the Kickapoo and southern Johnson Valley faults have a common history, supporting the suggestion (Sowers et al., 1994) *that they are essentially the same structure?* We have dated several surface ruptures on the northern Johnson Valley, southern Johnson Valley, and Kickapoo faults to test the idea that the southern Johnson Valley and Kickapoo faults are essentially the same structure, as suggested by Sowers *et al.* (1994). The penultimate event at all trench sites on northern and southern Johnson Valley and Kickapoo faults are indistinguishable at about 5 ka, within the bounds of uncertainty, and may represent the same event. However, the mean values of the age data suggest that the northern Johnson Valley fault failed up to several hundred years earlier than the Kickapoo or southern Johnson Valley faults. This would be a different pattern than the 1992 event, which did not rupture the northern extent of the Johnson Valley fault. Prior to the circa 5 ka event, each of these faults appears to have a different rupture history. The northern portion of the Johnson Valley fault also failed at about 7.3 ± 0.8 ka, apparently with less slip. The southern Johnson Valley fault also ruptured during the early Holocene, at approximately 10 ± 2 ka. Considering that the age ranges of these events barely overlap, it is plausible (but unlikely) that they are the same event. The Batdorf trench exhibited only three surface ruptures on the Kickapoo fault during the past 20 ka, with the prepenultimate event at about 18.5 ka. If the rupture history at the Batdorf site is complete, then the earlier events of the southern Johnson Valley fault between about 7 and 18 ka did not rupture the Kickapoo fault. These data suggest that each of these faults, although structurally linked, have a different rupture history. Considering this, we have chosen to preserve the adopted names of each of these fault segments. Nevertheless, the similarity in strike between the southern Johnson Valley and Kickapoo faults, along with the observation that they may rupture together in some events supports the contention of Sowers *et al.* (1994) that they are essentially the same fault.

Issue 4. What are the recurrence rates, and therefore the inferred slip rates, for faults along the 1992 rupture? One result that came out of this trenching is that the return time for surface ruptures at individual points along any and all of the faults involved in the 1992 earthquake is relatively long, on the order of 5–15 ka. This long return period is comparable to that for other faults studied after the earthquake, which also show correspondingly long recurrence intervals (Hecker *et al.,* 1993; Padgett and Rockwell, 1994; Bryan and Rockwell, 1995; Houser and Rockwell, 1996; Rubin and Sieh, 1997). We use the estimated return times for large displacement events on each of the faults studied to estimate a slip rate, assuming that slip was similar in prior events as in 1992. As discussed later, that assumption is generally supported by similar amounts of dip separation from event to event.

For the southern Johnson Valley fault, we have established an average return period of approximately 5 ka, which is consistent with the lapse time since the penultimate event. Using this interval and the ~3 m of slip measured along the southern Johnson Valley fault, we suggest a slip rate of about 0.6 mm/yr for this structure. Similarly, the Kickapoo fault has sustained three surface ruptures during the past 20 ka, with the penultimate event possibly larger than 1992. Nevertheless, assuming that they all exhibited about the same amount of strike slip, 2.5 m in 1992 at Bodick Road, and using an average return period of ~9 ka, we calculate a rate of about 0.2 mm/yr.

For the northern Johnson Valley fault, the data are less constrained so any slip-rate estimate is poor. Nevertheless, we have established that two significant surface ruptures have broken this fault during the past 11.5 ka, with possibly a third, smaller displacement at about 11.5 ka. The most recent event appears to have produced the most damage to the stratigraphy so we suspect that it was the largest. Beyond the mismatch in stratigraphy across the fault between trench walls (about 1 m), there are no constraints as to the amount of slip in the 5 ka event. Nevertheless, in that ~3 m seems to have been a fairly average amount of slip in the 1992 event, and Padgett and Rockwell (1994) established that the Lenwood fault has failed with 3-m slip events, we assume a similar amount (3 ± 1 m) for the most recent northern Johnson Valley event. For the 7.5 ka event, however, the rupture did not activate the entire width of the fault zone so it may have been smaller. From our observations, it is not likely that more than 6 m of slip has been released in the past 12 ka, suggesting a rate of less than 0.5 mm/yr. Future work should concentrate on resolving slip in past Mojave earthquakes, especially along the northern Johnson Valley fault where no data exist.

Resolving the slip rate on the Homestead Valley fault also is problematic due to the disparate records at the two trench sites. We speculate that only the large events, like 1992, activate the thrust faults at our Thrust site, although we allow that smaller events may have occurred for which we do not see any evidence. If most of the strain is released in these large events with about 3 m of slip, and our observations of about 5–6 events in the past 60–100 ka are valid, then a return period of 10–20 ka is estimated. Notably, the average recurrence interval of 15 ka is about how long it has been since the penultimate event. If all other slip events, such as the one recognized at the Playa site, are small (perhaps similar to the 1975 or 1979 events with centimeters of displacement), then the slip rate for the Homestead Valley fault is on the order of 0.15–0.3 mm/yr.

It is interesting to note that the Homestead Valley and Kickapoo faults have similar inferred rates at about 0.2 mm/yr, and that the southern Johnson Valley fault has the highest inferred rate at about 0.6 mm/yr. It is also interesting that the combined rates of the Homestead-Kickapoo trend and the northern Johnson Valley fault more or less equal that of the southern Johnson Valley fault. This suggests a relatively simple transfer of strain in this part of the ECSZ.

Issue 5. Finally, is there any evidence to suggest a change in the late Quaternary behavior or rate of earthquake occurrence that would indicate the development of a new system of faults, as suggested by Nur et al. *(1993a, 1993b) and Du and Aydin (1996)*? Our observations can, to some degree, test recent suggestions that there has been a change in the late Quaternary behavior or rate of earthquake occurrence that would indicate the development of a new system of faults, as suggested by Nur *et al.* (1993a, 1993b) and Du and Aydin (1996). They suggest that the northerly striking faults are "new" and now accommodate slip that had formerly occurred on the northwesterly striking set of faults. Part of this model suggests that the northwest-striking faults are now inactive, or becoming so.

It is plausible that the southern Johnson Valley fault has evolved over the past several hundred thousand years, although this is difficult to prove because there are no estimates of total slip across the fault. However, using our recurrence interval and inferred slip rate of 0.6 mm/yr, the expected amount of slip is small. The Homestead Valley fault has only a few hundred meters of total slip (Zachariasen and Sieh, 1995), and the northern Johnson Valley also has relatively little displacement with about a kilometer of right-lateral slip (Manson, 1986), so the total expected slip for the southern Johnson Valley is little more than a kilometer.

If the total slip for the southern Johnson Valley fault is simply the sum of the northern Johnson Valley and Homestead faults (about 1.3 km) and assuming that 0.6 mm/yr has been the slip rate since fault inception, then the age of the southern Johnson Valley fault would be about 2 Ma. This is similar to the ages (or perhaps older than) that Dokka and Travis (1990a) place on faults of the western Mojave desert. It does not support the hypothesis that northerly striking faults are newer than the northwest-striking ones. It is possible that the southern Johnson Valley fault has less slip than expected (<1.3 km), and that activity has propagated southward during the Quaternary. However, that does not really favor one model over another.

In summary, we see no evidence that the late Pleistocene to Holocene behavior has changed for any of the faults. In fact, none of the faults that we trenched have a relatively short recurrence interval that would indicate a significant slip rate. We observe that dextral shear is distributed across the Mojave shear zone, as previously inferred by Dokka and Travis (1990a, 1990b). The northerly striking faults have similar return periods to the northwest-striking faults and there has been no observable changes within the latest Quaternary. The return periods for 1992-type events are probably quite long in that we see no strong evidence for a prior combination of ruptures during the past 20 ka or so. We interpret our observations to mean that there have been no recent changes in fault behavior in the south part of the Mojave shear zone. Comparing the long and short-term activity of these faults, as inferred from the faults' total slip and our trenching, suggests that the last 20 ka of earthquake activity reflects the status quo for the ECSZ in southern California.

A surprising result from our work is that moment release in the western portion of the ECSZ appears to have clustered during the past 10–15 ka, with distinct bursts of seismic activity at 0–1 ka, 5–6 ka, and 9–10 ka. This may reflect a number of processes that are fundamental to our understanding of regional deformation such as episodic strain accumulation or episodic strain release due to the nature of the loading. Further work is certainly warranted in this region of infrequent, large earthquakes, both from a current seismic hazard perspective and to further our understanding of the physical processes involved in the generation of large earthquakes.

Acknowledgments

First and foremost, we thank the BLM and several landowners who granted land access and permission for trenching. We also thank the many SDSU students who participated in the trenching and logging as part of Rockwell's neotectonics classes. In particular, we thank Eldon Gath, Kim Thorup, Kevin Bryan, Mitch Bornyasz, and Monte Murbach who spent many days of their own time helping with various phases of this project. Earlier drafts of this paper were reviewed by James Dolan, Ray Weldon, and Lisa Grant, and their constructive reviews led to significant improvement of the presentation of this work. Research supported by the Southern California Earthquake Center, which is funded by NSF cooperative agreement EAR-8920136 and U.S. Geological Survey cooperative agreement 14-08-001-A0899 and 1434-HQ-97AG01718. The SCEC contribution number for this paper is 505.

References

Aitken, M. J. (1985). *Thermoluminescence Dating,* Academic, San Diego, 351 pp.

Aitken, M. J. (1998). *Introduction to Optical Dating,* Oxford U Press, Oxford, 256 pp.

Allen, C. R. (1975). Geological criteria for evaluating seismicity, *Geol. Soc. Am. Bull.* **86,** 1041–1057.

Berger, G. W. (1988). Dating Quaternary events by luminescence, in *Dating Quaternary Sediments,* D. J. Easterbrook (Editor), Geological Society of America Special Paper 227, 13–50.

Berger, G. W. (1995). Progress in luminescence dating methods for Quaternary sediments; *Dating Methods for Quaternary Deposits,* in N. W. Rutter and N. Catto (Editors), Geological Association of Canada, GEOtext no. 2, 81–103.

Birkeland, P. W. (1984). *Soils and Geomorphology,* Oxford U Press, New York, 348 p.

Bornyasz, M. S. (1993). Neotectonics of the Johnson Valley fault, Mojave Desert, California, unpublished Senior Thesis, Dept. of Geol. Sci., San Diego State University, 13 pp. + figures.

Bryan, K., and T. K. Rockwell (1994). Recognition of non-brittle fault deformation in trench exposures: an example from the Helendale fault, in *Mojave Desert: South Coast Geological Society Annual Fieldtrip Guidebook,* D. Murbach (Editor), Santa Ana, California, 253–262.

Bryan, K. A., and T. K. Rockwell (1995). Holocene character of the Helendale fault zone. Lucerne Valley, San Bernardino County, California, (abstracts with programs), *Geol. Soc. Am.* **27,** 7.

Buwalda, J. P., and C. F. Richter (1948). Movement of the Manix (California) fault on April 10, 1947, (abstract), Geol. Soc. Am. Bull. **59,** 1367.

Cinti F. R., T. E. Fumal, C. D. Garvin, J. C. Hamilton, T. J. Powers, and D. P. Schwartz (1993). Earthquake recurrence and fault behavior on the Homestead Valley fault—central segment of the 1992 Landers surface rupture sequence (abstracts with programs), Geol. Soc. Am. **25,** 101.

Crippen, R. (1988). Southerly continuation of the Johnson Valley fault, east of the San Bernardino Mountains, southern California (Abstracts with programs), *Geol. Soc. Am. Bull.,* **20,** 152–153.

Dijkerman, J. C., M. G. Cline, and G. W. Olson (1967). Properties and genesis of textural subsoil lamellae, *Soil Science* **104,** 7–16.

Dokka, R. K. (1983). Displacements on late Cenozoic strike-slip faults of the central Mojave Desert, California, *Geology* **11,** 305–308.

Dokka, R. K., and C. J. Travis (1990a). Late Cenozoic strike-slip faulting in the Mojave Desert, California, *Tectonics* **9,** 311–340.

Dokka, R. K., and C. J. Travis (1990b). Role of the eastern California shear zone in accommodating Pacific-North American plate motion, *Geophys. Res. Lett.* **17,** 1323–1326.

Du, Y., and A. Aydin (1996). Is the San Andreas big bend responsible for the Landers earthquake and the eastern California shear zone?, *Geology* **24,** 219–222.

Eghbal, M. K., and R. J. Southard (1993). Stratigraphy and genesis of Durorthids and Haplargids on dissected alluvial fans, western Mojave Desert, California, *Geoderma* **59,** 151–174.

Gile, L. H., J. W. Hawley, and R. B. Grossman (1981). Soils and geomorphology in the Basin and Range area of southern New Mexico—Guidebook to the Desert Project, New Mexico Bureau of Mines and Mineral Resources Memoir 39, 222 pp.

Hart, E., W. A. Bryant, J. E. Kahle, M. W. Manson, and E. J. Bortugno (1988). Summary report: fault evaluation program 1986–1987, Mojave Desert and other areas, *California Division of Mines and Geology, Open File Report 88-1,* 40 pp.

Hart, E. W., W. A. Bryant, and J. A. Treiman (1993). Surface faulting associated with the June 1992 Landers earthquake, California, *California Geology,* **46,** 10–16.

Hecker, S., T. E. Fumal, T. J. Powers, J. C. Hamilton, C. D. Garvin, and D. P. Schwartz (1993). Late Pleistocene-Holocene behavior of the Homestead Valley fault segment—1992 Landers, CA surface rupture, *EOS AGU Fall Supplement,* 612.

Herzberg, M., and T. K. Rockwell (1993). Timing of past earthquakes on the northern Johnson Valley fault and their relationship to the 1992 rupture, *EOS AGU Fall Supplement,* 612.

Herzberg, M. (1996). The neotectonic history of the Johnson Valley fault, San Bernardino County, California, *M.S. Thesis,* San Diego State University, 68 pp.

Houser, C. E. (1996). Tectonic geomorphology and Quaternary history of the Old Woman Springs fault, San Bernardino County, California, *M.S. Thesis,* San Diego State University, 81 pp.

Houser, C. E. and T. K. Rockwell (1996). Tectonic geomorphology and paleoseismology of the Old Woman Springs fault. San Bernardino County, California (abstracts with programs), *Geol. Soc. Am.* **28,** 76.

Huntley, D. J., D. I. Godfrey-Smith, and E. H. Haskell (1991). Light-induced emission spectra from some quartz and feldspars, *Nuclear Tracks and Radiation Measurements* **18,** 127–131.

Jennings, C. W. (1975). Fault map of California, California Geologic Data Map Series, Map No. 1, California Division of Mines and Geology.

Kanamori, H., H. K. Thio, D. Dreger, E. Hauksson, and T. Heaton (1992). Initial investigation of the Landers, California, earthquake of 28 June, 1992 using TERRAscope, *Geophys. Res. Lett.* **19,** 2267–2270.

Knuepher, P. L. K. (1989). Implications of the characteristics of end-points of historical surface fault ruptures for the nature of fault segmentation, in *Fault Segmentation and Controls of Rupture Initiation and Termination,* D.P. Schwartz and R. Sibson (Editors), *U.S. Geol. Surv. Open-File Rept. 89-315,* 409–431.

Lamothe, M., and M. Auclair (1999). A solution to anomalous fading and age shortfalls in optical dating of feldspar minerals, *Earth and Planetary Science Letters* **171,** 319–323.

Lazarte, C. A., J. D. Bray, A. M. Johnson, and R. E. Lemmer (1994). Surface breakage of the 1992 Landers Earthquake and its effect on structures, *Bull. Seism. Soc. Am.* **84,** 547–561.

Lian, O. B., and D. Huntley (1999). Optical dating studies of post-glacial aeolian deposits from the south-central interior of British Columbia, Canada, *Quaternary Science Reviews* **18,** 1453–1466.

Lindvall, S. C., and T. K. Rockwell (1993). Recurrent Holocene faulting along the Johnson Vall. portion of the 1992 Landers earthquake surface rupture (abstracts with programs) *Geol. Soc. Am.* **25,** 70.

Lindvall, S. C., and T. K. Rockwell (1994). Continuing paleoseismic studies along the southern 1992 Landers earthquake rupture (abstracts with programs); *Geol. Soc. Am.* **26,** 67.

Machette, M. N. (1985). Calcic soils of the southwestern United States, in L. D. Weide (Editor), *Soils and Quaternary Geology of the Southwestern United States, Geol. Soc. Am. Special Paper 203,* 1–22.

Manson, M. W. (1986). Fault evaluation report for the Homestead Valley fault, Johnson Valley fault, and associated faults, San Bernardino County, FER 180, California Division of Mines and Geology, Sacramento, 10 pp. plus maps.

McFadden, L. D. (1988). Climatic influences on rates and processes of soil development in Quaternary deposits of southern California, *Paleosols and Weathering Through Time: Principals and Applications,* J. Reinhardt and W. R. Sigleo (Editors), *Geol. Soc. Am. Special Paper 206,* 153–177.

Murbach, D., T. K. Rockwell, and J. D. Bray (1999). The relationship of foundation deformation to surface rupture and near-surface faulting resulting from the 1992 Landers earthquake, *Earthquake Spectra* **15,** no. 1, 121–144.

Nur, A., H. Ron, and G. Beroza (1993a). The nature of the Landers-Mojave earthquake line, *Science* **261,** 201–203.

Nur, A., H. Ron, and G. Beroza (1993b). Landers-Mojave earthquake line: A new fault system?, *GSA Today* **3,** 253, 256–258.

Ollerhead, J., D. J. Huntley, and G. W. Berger (1994). Luminescence dating of the Buctouche Spit, New Brunswick, *Canadian Journal of Earth Sciences* **31,** 523–531.

Padgett, D. C., and T. K. Rockwell (1994). Paleoseismology of the Lenwood fault, San Bernardino County, California, in *Mojave Desert: South Coast Geological Society Annual Fieldtrip Guidebook,* D. Murbach (Editor), 222–238.

Reheis, M. C., J. W. Harden, L. D. McFadden, and R. R. Shroba (1989). Development rates of late Quaternary soils, Silver Lake Playa, California, *Soil Science Society of America* **32,** 1127–1139.

Rockwell, T. K. (1998). Use of soil geomorphology in fault studies, in *Quaternary Geochronology: Applications in Quaternary Geology and Paleoseismology* J. S. Noller, J. M. Sowers, and W. R. Lettis (Editors), NUREG series publication, U.S. Nuclear Regulatory Commission.

Rockwell, T. K., D. P. Schwartz, K. E. Sieh, C. Rubin, S. Lindvall, M. Herzberg, D. Padgett, and T. Fumal (1993). Initial paleoseismic studies following the Landers earthquake: implications for fault segmentation and earthquake clustering, *EOS AGU Fall Supplement,* 67.

Rubin, C. M., and K. Sieh (1997). Long dormancy, low slip rate, and similar slip-per-event for the Emerson fault, eastern California shear zone, *J. Geophys. Res.* **102,** 15319–15333.

Rubin, C. M., S. C. Lindvall, and T. K. Rockwell (1998). Evidence for large earthquakes in metropolitan Los Angeles, *Science* **281,** 398–402.

Sauber, J., W. Thatcher, and S. C. Solomon (1986). Geodetic measurements of deformation in the central Mojave Desert, California, *J. Geophys. Res.* **91,** 12683–12693.

Scientists from the USGS, SCEC and CDMG (2000). Preliminary report on the 16 October 1999 *M* 7.1 Hector Mine, California, earthquake, *Seism. Res. Lett.* **71,** 11–23.

Sibson, R. H. (1985). Stopping of fault ruptures at dilational fault jogs, *Nature* **316,** 248–251.

Sieh, K., L. Jones, E. Hauksson, K. Hudnut, D. Éberhart-Phillips, T. Heaton, S. Hough, K. Hutton, H. Kanamori, A. Lilje, S. Lindrall, S. McGill, J. Mori, C. Rubin, J. Spotila, J. Stock, H. K. Thio, J. Treiman, B. Wernicke, and J. Zachariasen (1993). Near-field investigations of the Landers earthquake sequence, April to July, 1992, *Science* **260,** 171–176.

Soil Survey Staff (1991). Soil Survey Manual, Government Printing Office, Washington, D.C., 732 pp.

Soil Survey Staff (1992). *Keys to Soil Taxonomy,* U.S.D.A., SMSS Technical Monograph No. 19, Pocahontas Press, Blacksburg, Virginia, 541 pp.

Sowers, J. M., J. R. Unruh, W. R. Lettis, and T. D. Rubin (1994). Relationship of the Kickapoo fault to the Johnson Valley and Homestead Valley faults, San Bernardino County, California, *Bull. Seism. Soc. Am.* **84,** 528–536.

Torrent, J., W. D. Nettleton, and G. Borst (1980). Clay illuviation and lamella formation in a psammentic haploxeralf in Southern California, *Soil Science Soc. Am. J.* **44,** 363–369.

Vaughan, P. R., K. M. Thorup, and T. K. Rockwell (1999). Paleoseismology of the Elsinore fault at Agua Tibia Mountain, southern California, *Bull. Seism. Soc. Am.* **89,** 1447–1457.

Wells, D. L., and K. J. Coppersmith (1994). New emperical relationships among magnitude, rupture length, rupture width, rupture area, and surface displacement, *Bul. Seism. Soc. Am.* **84,** 974–1002.

Zachariasen, J., and K. Sieh (1995). The transfer of slip between two en eschelon strike-slip faults: a case study from the 1992 Landers earthquake, southern California, *J. Geophys. Res.* **100,** 15281–15301.

Appendix

Dating Methods

We used four dating techniques to constrain the ages of alluvial deposits in our studies: soil geomorphology, thermoluminescence (TL) and proton-stimulated-luminescence

(PSL) dating of fine-grained and sandy sediments, and conventional radiocarbon dating on detrital charcoal. Each of the techniques provides largely independent assessments of age, and each therefore help constrain the actual age of alluvial deposits. We use the radiocarbon, TL and PSL dates to constrain the ages of some of the soil units described in this study, so the soil age estimates are not completely independent of the other techniques.

Soil Dating. Soil, in the context of our study, is the weathering profile that develops at the Earth's surface due to physical and chemical changes that occur over time (Birkeland, 1984; Rockwell, 1998). It is the time element or factor in soil formation that we use to assess the ages of faulted and unfaulted deposits, and for correlation of deposits across faults. A sequence of soils that vary as a function of their ages is termed a soil chronosequence. If independent age control can be determined for some chronosequence members, or if the soils can be correlated to dated soils elsewhere that have developed under similar climatic conditions and in similar parent materials, we can also use those dated soils to help constrain the ages of undated profiles in our study.

Previous soil studies in the Mojave region include development of chronosequences (McFadden, 1988; Reheis *et al.,* 1989; Herzberg, 1996), as well as more general studies of soil genesis (Machette, 1985; Eghbal and Southard, 1993). We include the data from these previous studies, along with independently dated soil data from our studies, to provide calibration for undated soils described herein.

About 40 pedons were described in alluvial deposits along the 1992 rupture (Herzberg, 1996) according to guidelines set forth by the USDA Soil Conservation Service (Birkeland, 1984, Soil Survey Staff, 1991, 1992). Ten of these pedons are used in this study (Table 1)). Samples were collected from many of the described pedons and analyzed for particle size distribution, bulk density, and carbonate content, where appropriate. Many of the soil exposures were backhoe trenches used to expose the fault during the paleoseismic studies. We also utilized natural and road-cut exposures where necessary.

The older (Pleistocene) soils can be generally separated into two groups: Argids (those with argillic horizons and little or no calcium carbonate) near the range-front of the San Bernardino Mountains and Orthids (those with calcium carbonate and little or no translocated clay) farther out into the Mojave Desert. The Holocene soils are generally very weak and display little to no pedogenic development. These observations indicate that a substantial rainfall gradient existed during the late Pleistocene near the range-front out onto the desert floor and that the expression of the soil in deposits of a common age may vary as a function of the local paleoclimate.

In this study, the significance of the expression of individual soil profiles is discussed in the context of the fault relationships at each trench site, as applicable. For some soils, we can make rather strong estimates of their ages, based on comparison to well-dated soils elsewhere in the Mojave region. In others, comparable dated soils are few and the soil age estimates are poorly constrained. In each case, however, the soils have been useful in helping to constrain and interpret the faulting relationships, even where errors on the age estimates are large.

Thermoluminescence and PSL Dating. Under ideal conditions, TL and PSL dating techniques measure the time since the sediments were last exposed to daylight, and therefore the time since their burial. We collected and analyzed 28 samples (21 samples as presented in Table 2 and an additional seven samples for zeroing tests, with detailed results to be described elsewhere) to determine ages of some of the soils and faulted alluvial deposits in this study. For TL dating, we measured the blue-UV emission, which arises from both feldspar and quartz, but dominantly from feldspar. For PSL dating, we used 1.4 eV (880 nm, near-infrared) excitation and measured the 3.1 eV (400 nm, violet) emission characteristic of K-feldspars (Aitken, 1998; Huntley *et al.,* 1991; Ollerhead *et al.,* 1994). Both methods are based on the observation that during radioactive decay occurring in the sample and its surroundings, some of this radiation energy is stored in the mineral grains of the sediment. The energy is stored in the mineral lattice partly as a potential energy of "trapped" electrons. The rate at which radiation energy is absorbed is called the dose rate and is a function of the concentration of radioactive elements present within the sample and in the soil immediately around it (up to about a 30-cm radius). The longer the exposure to the radiation, the greater the luminescence measured later in the laboratory when the trapped electrons are released by heat, in the case of TL, or light, in the case of excitation by photons.

An important distinction between the techniques is that in TL dating all the trapped electrons are sampled, both light-sensitive and light-insensitive, while in PSL dating only light-sensitive trapped electrons are released. Daylight exposure just prior to sediment burial releases electrons from traps, thereby resetting the clock. Alluvial material in which each grain has been exposed to many hours of direct sunlight will still yield a measurable "residual" or relict TL, which arises from light-insensitive electron traps, and the dating technique corrects for this. In contrast, grains exposed to only a few minutes of direct sunlight yield a usually negligible luminescence under photon excitation. The ideal sample is one which was very well exposed to daylight before burial, in which case both techniques should yield the same age. Conversely, if both techniques yield the same age then the sample was well bleached prior to burial. Possibly the daylight exposure could be such that PSL dating would give the correct age, but TL dating would give an incorrectly high age. With the multialiquot procedures that we used, if some grains were not bleached at all, but some were, the measured age from both methods would be a maximum for the age of deposition. This can occur, for example, if some grains were clumped or shielded by a coating during transport, or if some were transported during darkness, such as at night or in a sandstorm (Aitken, 1985, 1998; Berger, 1988, 1995; Lian and Huntley, 1999).

To assess the potential utility of these dating techniques in the study area and for the alluvial materials generally present in our trench exposures, we tested the adequacy of the daylight exposure by collecting and measuring three surface samples. In the area of the Hondo trench site along the southern Johnson Valley fault, we collected soil material from a ground squirrel midden and from the topmost 4 cm of sediment on the 1992 scarp face. The ground squirrel midden material was an important test because there is abundance evidence for squirrel activity around the Hondo trench site and this activity may be a significant cause of mineral grains becoming exposed to daylight. We also collected material from a two-month-old ant mound in Homestead Valley. Of the three samples, the zeroing test on the scarp face sample is perhaps the most important such test because this material is presumably the source material for the colluvium shed from the scarp after an earthquake.

The results of these tests showed that zero-age samples from this area are likely to yield apparent TL ages of 500 $\pm$ 100 years and apparent PSL ages of 50 $\pm$ 20 years. Consequently, 500 years has been subtracted from the calculated TL dates on samples recovered from the trench stratigraphy to better constrain the actual ages of the respective deposits (Table 2). In the text these are listed as "corrected" ages, rounded to the closest 0.1 ka, with the analytical laboratory errors rounded up to the nearest 0.1 ka. No such subtraction was made for the PSL ages.

All of the foregoing assumes that the measured signals from the feldspars contain no significant uncorrected anomalous-fading component. Certain feldspars, notably those from volcanic regions (Aitken, 1985, 1998) have an unstable signal that cannot be removed by laboratory preheating, such as we employed here (Berger, 1994; Ollerhead *et al.,* 1994). However, as mentioned in the text (Melville Gap site), there is widespread evidence that significant age underestimation arising from uncorrected anomalous fading is a regional effect, that it is less serious for multialiquot samples than for single-aliquot and single-grain samples, and that our study region is not likely to yield multialiquot samples having this problem. Furthermore, it is unlikely that such an effect would be as dramatic in Holocene ^{14}C dates reported in our text for the Melville Gap site.

Department of Geological Sciences
San Diego State University
San Diego, California 92182
(T. K. R., T. D.)

William Lettis & Associates, Inc.
25050 Avenue Kearny, Suite 108
Valencia, California 91355
(S. L.)

Earth Consultants International
3934 Murphy Canyon Rd., #B-104
San Diego, California 92123
(T. K. R., M. H., D. M.)

Quaternary Science Center
Desert Research Institute
P.O. Box 60220
Reno, Nevada 89506-0220
(G. B.)

Manuscript received 1 March 1999.